CHARACTERIZING PAVEMENT SKID RESISTANCE FOR ROADWAY CRASH PREDICTION IN OKLAHOMA

By

WENYING YU

Bachelor of Science in Civil Engineering

Oklahoma State University

Stillwater, Oklahoma

2017

Submitted to the Faculty of the
Graduate College of the
Oklahoma State University
in partial fulfillment of
the requirements for
the Degree of
MASTER OF SCIENCE
July, 2019

CHARACTERIZING PAVEMENT SKID

RESISTANCE FOR ROADWAY CRASH PREDICTION

IN OKLAHOMA

Thesis Approved:

Dr. Qiang Joshua Li

Thesis Adviser

Dr. Kelvin C.P. Wang

Dr. Stephen Alan Cross

ACKNOWLEDGEMENTS

This thesis was prepared under two research projects, “Continuous Friction Measurement Equipment (CFME) for Highway Safety Management in Oklahoma”, and “Utilizing Pavement Friction and Texture Data for the Reduction of Traffic Crashes and Delays”, sponsored by the Oklahoma Department of Transportation (ODOT). Special thanks are due to ODOT for both financial and technical support and providing relevant data for the study. Special thanks also go to the OSU research team for their assistances in collecting and preprocessing field data and providing valuable feedback. Moreover, I would like to express my profound gratitude to my adviser, Dr. Qiang Joshua Li, for allowing me to contribute in the research projects, and his guidance and patience throughout my master’s study and research. Thanks also go to the committee members, Dr. Kelvin C.P. Wang and Dr. Stephen Alan Cross, for the willingness to serve on the committee and their technical guidance of this thesis research. Finally, I must express thanks to my family, for their continuous supports and encouragements throughout my years of study. This thesis would not have been possible without any of them.

Name: WENYING YU

Date of Degree: JULY, 2019

Title of Study: CHARACTERIZING PAVEMENT SKID RESISTANCE FOR ROADWAY CRASH PREDICTION IN OKLAHOMA

Major Field: CIVIL ENGINEERING

Abstract: Skid resistance is critical for roadway safety. This study investigates two approaches to characterizing skid resistance based on pavement texture data and further exploring its effects on roadway crashes in Oklahoma. Skid resistance data were acquired in the field from three friction measurement devices: Grip Tester, a continuous friction measurement equipment (CFME), dynamic friction tester (DFT), and a locked wheel skid trailer. While pavement texture data were obtained using a high-speed profiler and a portable 3D laser scanner with ultra-high resolution. Through a comprehensive field data collection on testing sites with different preventive maintenance treatments in Oklahoma, this study evaluates the repeatability and the impacts of various operational factors on Grip Tester based CFME measurements. An adaptive signal processing technique, Hilbert-Huang transformation, is executed to extract texture characteristics from pavement profiles, which are subsequently correlated to friction measurements. Novel 3D areal texture parameters are calculated at both micro- and macro- scales. The random forest algorithm is implemented to determine the most important texture parameters for the development of friction prediction models. On the other hand, skid resistance and roadway features could have critical effects on highway safety but have not been fully considered to estimate crash rates in the current HSM safety performance functions (SPFs). In this study, four database systems managed by the Oklahoma DOT are utilized to integrate various safety-related roadway features into the SPF development process. Roadway crash data, pavement skid resistance, pavement management system (PMS) condition data, and traffic data from 2012 to 2016 in Oklahoma were acquired for the interstate, selected U.S. and state highways. An enhanced SPF is subsequently developed using negative binomial regression model with a log-linear relationship between crash frequency and roadway features. It is anticipated the work in this study could assist in well-informed decision making in terms of roadway safety for pavement preservation and maintenance practices in Oklahoma.

TABLE OF CONTENTS

Chapter Page

LIST OF TABLES

Table Page

LIST OF FIGURES

Figure Page

CHAPTER I

INTRODUCTION

Problem Statement

Safety is one of the top priorities of the U. S. Department of Transportation (DOT). According to a study by Federal Highway Administration (FHWA, 2018), traffic crashes resulted in approximately 37,150 fatalities in 2017, or 1.17 fatalities per 100 million vehicle miles traveled. Various influencing factors could contribute to the traffic crashes, including the human behavior, the vehicle, the environment and the roadway (HSM, 2010). Of all these factors, skid resistance is critically important as it keeps vehicles on the road by allowing drivers to control or maneuver their vehicle (Hall et. al, 2009). It was found that about 70 percent of wet pavement crashes could be prevented or minimized by improved pavement friction (FHWA, 2016).

Pavement skid resistance can be typically characterized by tire-pavement friction, macro- and micro- texture of the pavement surface. The field friction testing methods can be categorized into four groups: locked-wheel, side-force, variable-slip, and fixed-slip (Hall et al., 2009). The last three types of devices are generally characterized as continuous friction measurement equipment (CFME). Currently, most State Highway Agencies (SHAs), including the Oklahoma Department of Transportation (ODOT), employ locked-wheel skid trailers for friction measurements at the network scale (Henry, 2000). In recent years, CFME is recommended as a more appropriate method for pavement friction measurement (FHWA, 2010). CFME has the capability to continuously measure surface friction, providing greater details about spatial variability of the

tire-pavement frictional properties (Flintsch et al., 2012). Moreover, unlike the locked wheel method by fully braking the testing tire used in the 1950s vehicle braking technology, CFME simulates the modern anti-braking system (ABS) equipped on current vehicles with a slip ratio of the testing tire during data collection. In addition, it consumes less water as compared with a locked-wheel skid trailer. However, due to the lack of practices at this time, research is needed to evaluate the repeatability of CFME and understand its response to various operational characteristics.

It is commonly agreed that friction is dominated by micro-texture (<0.5 mm) and macro-texture (0.5 mm~50 mm) of pavement surface (Flintsch et. al, 2012; Henry, 2000; Kogbara et al., 2016). Unlike friction measurement using contact-based method, pavement or aggregate surface texture can be characterized at both micro- and macro- scales using high resolution non-contact measurement methods. Many research projects have made efforts in studying the relationship between friction and texture so that the measurement of friction can be enhanced or replaced by non-contact texture based measurements with the advancement of sensor technologies. However, the correlations between friction and texture indicators are not consistent among various studies (Flintsch et al., 2012; Hall et al., 2008; Kargah-Ostadi et al., 2015). Various texture parameters in disciplines other than pavement engineering are available for surface texture characterization and evaluation, which provide an alternative approach to studying the friction-texture relationship.

Roadway safety is evaluated and estimated by the crash frequency in the Highway Safety Manual (HSM, 2010). The HSM provides an approach that utilizes regression equations, the Safety Performance Functions (SPFs), to predict the crash frequency for a specific site type. Although skid resistance is well known to be one of the contributing factors of crash, it is not considered in the current SPFs. Highway agencies are encouraged to develop state-specific SPFs for different roadway facilities and crash types (Merritt et al., 2015). Oklahoma Department of Transportation (ODOT) collects and manages safety-related data for the entire pavement networks for many

years. The available databases offer valuable resources for the development of enhanced SPF for more accurate roadway crash prediction and thus more robust pavement friction management.

Thesis Objectives

The objectives of the thesis include:

1. Evaluating the Grip Tester based CFME measurements.
    a. The repeatability of Grip Tester measurements on different types of surface for both concrete and asphalt pavements.
    b. The influence of different operational characteristics on Grip Tester measurements by a comprehensive statistical model.
    c. The feasibility of a signal processing method, Hilbert-Huang Transformation (HHT), to characterize and quantify pavement surface texture.
2. Developing pavement friction prediction models using high-resolution 3D texture data.
    a. Identify the suitable 3D areal pavement texture parameters at both micro- and macro- scales for surface texture characterization.
    b. Develop friction prediction models at both high and low speeds.
3. Developing enhanced SPF for highway segments in Oklahoma.
    a. Identify the potential influencing factors, including skid resistance and roadway characteristics, for safety analysis and compile their data from various ODDT database systems.
    b. Determine whether these factors are significant for crash estimation.
    c. Develop enhanced SPF by integrating the significant influencing factors.
    d. Improve crash estimation using the Empirical Bayes method to reduce the regression-to-the-mean (RTM) bias.

Thesis Outline

This thesis is organized into six chapters.

Chapter 1: Introduction, illustrates the background and purpose of the thesis, including the Problem Statement, Thesis Objectives, and Thesis Outline.

Chapter 2: Review of Literature, explains the key concept of skid resistance, its critical importance to roadway safety and current practice of safety evaluation.

Chapter 3: Evaluation of Grip Tester Based Continuous Friction Measurement Equipment (CFME), evaluates the repeatability and the influencing factors of Grip Tester measurements.

Chapter 4: Random Forest Based Pavement Friction Prediction Using High-Resolution 3D Image Data, explores the relationship of friction and pavement texture and develops models for friction prediction using 3D areal texture parameters at both micro- and macro- scales.

Chapter 5: Enhanced Safety Performance Function for Highway Segments in Oklahoma, identifies the statistically significant factors for crash estimation and builds an enhanced Safety Performance Function by integrating influencing roadway characteristics.

Chapter 6: Conclusion, outlines the major findings through Chapter 3 to 5 and discusses the future work.

CHAPTER II

REVIEW OF LITERATURE

Pavement Friction Management

Roadway crash is one of the leading causes of death in United States. Each year, over 37,000 lives and 230.6 billion dollars are lost in the U.S. (ASIRT, 2018). Various influencing factors could contribute to the traffic crashes, including the human behavior, the vehicle, the environment and the roadway (HSM, 2010). Of all these factors, transportation engineers can control only the roadway features. It is widely agreed that the lack of sufficient tire-pavement friction could increase the risk of traffic crashes (Merritt and Zaloshnja, 2015; Najafi et al., 2017). Therefore, Federal Highway Administration (FHWA) issues guidance to State and local highway agencies in management of pavement surface friction on roadways.

The most recent Technical Advisory 5040.38: Pavement Friction Management, was issued in June 2010 (FHWA, 2010), superseding the previous Technical Advisory 5040.17: Skid Accident Reduction Program dated 1980. The goal of the new advisory (FHWA, 2010), is to minimize friction-related vehicle crashes by ensuring that pavements provide adequate and durable friction properties throughout their service lives in a cost-effective manner. It encourages agencies to utilize pavement friction and friction-related data, crash data and traffic data in an effective PFM program.

An important part of the PFM is the selection of the most appropriate friction measurement equipment. The new advisory lists four types of full-scale friction test equipment: the locked-

wheel, fixed slip, side force, and variable slip. The locked-wheel method (ASTM E-274, 2015) is widely used on U.S. highways and simulates emergency braking without anti-lock brakes. The three remaining methods can be characterized as continuous friction measurement equipment (CFME), which greatly enhance the ability to detect isolated low friction areas on pavements (de León Izeppi et al., 2016). In recent years, CFME is recommended as a more appropriate method for pavement friction measurement (FHWA, 2010). In addition, because all friction test methods can be insensitive to macro-texture under specific circumstances, it is recommended that friction testing be complemented by macro-texture measurement (FHWA, 2010).

The study of NCHRP Project 01-43 (2009) provides a comprehensive PFM program framework in *Guide for Pavement Friction*, which comprised of the following key components:

- Network Definition—subdivide the highway network into distinct pavement sections and group the sections according to levels of friction need.
    - Define pavement sections.
    - Establish friction demand categories.
- Network-Level Data Collection—Gather all the necessary information.
    - Establish field testing protocols (methods, equipment, frequency, conditions, etc.) for measuring pavement friction and texture.
    - Collect friction and texture data and determine overall friction of each section.
    - Collect crash data.
- Network-Level Data Analysis—Analyze friction and/or crash data to assess overall network condition and identify friction deficiencies.

    - Establish investigatory and intervention levels for friction. Investigatory and intervention levels are defined, respectively, as levels that prompt the need for a detailed site investigation or the application of a friction restoration treatment.
    - Identify pavement sections requiring detailed site investigation or intervention.

- Detailed Site Investigation—Evaluate and test deficient pavement sections to determine causes and remedies.
    - Evaluate non-friction-related items, such as alignment, the layout of lanes, intersections, and traffic control devices, the presence, amount, and severity of pavement distresses, and longitudinal and transverse pavement profiles.
    - Assess current pavement friction characteristics, both in terms of micro-texture and macro-texture.
    - Identify deficiencies that must be addressed by restoration.
    - Identify uniform sections for restoration design over the project length and schedule friction restoration activities as part of overall pavement management process.

- Selection and Prioritization of Short- and Long-Term Restoration Treatments—Plan and schedule friction restoration activities as part of overall pavement management process.
    - Identify candidate restoration techniques best suited to correct existing pavement deficiencies.
    - Compare costs and benefits of the different restoration alternatives over a defined analysis period.

- Consider monetary and non-monetary factors and select one pavement rehabilitation strategy.

In summary, the PFM program calls for routine friction testing of the roadway network, subsequent analysis of the data to identify friction deficiencies and final countermeasures to improve the safety. Agencies and researchers have implemented a wide variety of studies and practices to support the PFM program. Many States have installed the High Friction Surface Treatment (HFST) on spots with higher friction demands (FHWA, 2019), including Oklahoma, Kansas, Missouri, etc. The HFST involves the application of very high-quality aggregates, which has been verified to immediately reduce crashes, injuries, and fatalities associated with friction demand issues (FHWA, 2019; Zahir et al., 20170; Bledsoe, 2015). In order to better address the contribution of friction on highway safety, the Virginia Department of Transportation (DOT) integrates the skid resistance into the current crash prediction model. VDOT tests the skid resistance by a locked-wheel tester on all interstate and the primary routes on a multiyear cycle, doing two to three districts per year (de León Izeppi et al., 2016). Oklahoma DOT manages the Skid Studies Program, which used to perform systematic skid studies for the entire highway system, while in recent years the scope has been downsized to only include annual testing of US-69, all Interstate Highways, as well as the Strategic Highway Research Program (SHRP) sites. In addition, ODOT also conducts special skid resistance testing as requested (ODOT, 2018).

Pavement Skid Resistance

Pavement skid resistance is the force generated between a vehicle tire and a pavement surface (Austroads, 2011). It is critical for roadway safety as it keeps vehicles on the road by allowing drivers to control or maneuver their vehicle (Hall et al., 2009). In addition, it is a key factor in highway geometric design as it used for determining the adequacy of the minimum stopping sight distance, and minimum horizontal radius, etc.

Pavement skid resistance can be typically characterized by tire-pavement friction, macro- and micro- texture of the pavement surface. Figure 1 visualizes the interaction between texture and a wet pavement, which is named as Three Zone Concept and first suggested by Gough and later extended by Moore (Moore, 1966). In zone 1, water is squeezed out by the macro-texture of the pavement surface, whereas in zone 2, it is by micro-texture. In zone 3, the tire comes into dry contact with the pavement surface, where the forces of adhesion and hysteresis come into play. Adhesion and hysteresis are the two main components of tire-pavement friction. Adhesion is due to the molecular bonding between the tire and the pavement surface while hysteresis is the result of energy loss due to tire deformation. Both hysteresis and adhesion are related to surface characteristics and tire properties (Hall et al., 2009).

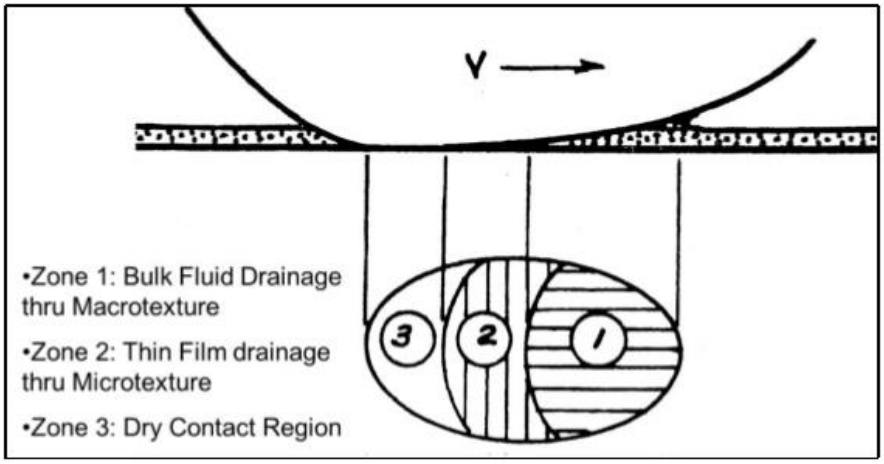

Figure 1 Texture Three Zone Concept of a Wet Surface (after Moore, 1966)

The skid resistance is usually quantified using the non-dimensional friction coefficient, μ as the ratio of the dragging force to the perpendicular force:

$$\mu = F/F_W \qquad (1)$$

It is worth noted that as the result of the interaction between the tire and the pavement, pavement friction depends on properties of both the road and the tire, with climatic factors also having an influence (Roe and Sinhal, 1998). It is dominated by the texture of pavement surface, mainly depending on the micro- and macro- texture, while mega-texture and unevenness are negligible

(Flintsch et al., 2012; Henry, 2000; Kogbara et al., 2016). Pavement texture is defined as "the deviations of the pavement surface from a true planar surface" in the NCHRP Project 01-43 *Guide for Pavement Friction* (Hall et al., 2009). Based on the wavelength of the deviations, the Permanent International Association of Road Congress (PIARC, 1987) defines the pavement texture into four types: micro-texture (<0.5 mm), macro-texture (0.5 mm~50 mm), mega-texture (50 mm~500 mm), and unevenness (>500 mm).

Table 1 Micro/macro Texture Ranges and Control Factors (Austroads, 2011)

Pavement Surface Texture	Texture Wavelength	Major factors controlling texture level	
		Asphalt surfacing	Seal surfacing
Micro-	<0.5mm	Selection of aggregate type (e.g. glassy, rough)	Selection of aggregate type (e.g. glassy, rough)
Macro-	0.5~50mm	Mix type and design (e.g. maximum aggregate size, grading control, binder content)	Seal type and design (e.g. seal size, binder application rate)

Micro-texture is the fine-scale surface texture of coarse aggregates in asphalt mixes or sands in cement concrete, which interacts directly with the tire rubber on a molecular scale and provide friction (Flintsch et al., 2012). It is a more inherent characteristic of the aggregates and thus determined by the aggregate source (Austroads, 2011). This component of texture is especially important to friction performance at low speeds but needs to be present at any speeds (Flintsch et al., 2012).

On wet pavements, as speed increases, skid resistance decreases and the extent to which this occurs depends on the macro-texture, typically formed by shape and size of the aggregate particles in the surface or by grooves cut into some surfaces (Austroads, 2011). Macro-texture can be controlled by the surfacing type selection and the mix/seal design. Generally, surfaces with greater macro-texture have better skid resistance at high speeds for the same low-speed skid

resistance (Roe and Sinhal, 1998). However, it worth noted that good skid resistance is not guaranteed by good texture (Merritt et al., 2015).

Measurement of Skid Resistance

The commercially available measurement devices obtain skid resistance using a rubber slider or tire being forced to slide across the wetted pavement surface (Austroads, 2011). The horizontal friction force resisting the sliding is measured, and the perpendicular force is either measured or assumed to be constant (Austroads, 2005).

The American Society for Testing and Materials (ASTM) sets the standards for operating and calibrating the equipment used for measuring skid resistance for most of the methods used in the U.S. The methods can be grouped into two categories: high-speed friction measurement, and low-speed or stationary friction measurement (Hall et al., 2009).

Low-Speed and Stationary Friction Measurements

Two devices that are typical for industrial and research use in the lab or at low speed in the field are the British Pendulum Tester (BPT) and the Dynamic Friction Tester (DFT),

British Pendulum Tester (BPT)

The BPT (Figure 2) has been in use since the early 1960s (Henry, 2000). The BPT (ASTM, 2018) is operated by releasing a pendulum from a specified height so that measures the energy loss when the rubber slider edge is propelled over a test surface. The slip speed for the BPT is typically assumed to be 10km/h (6mph). The difference between the height before the release and the height recovered is equal to the loss of kinetic energy due to the friction between slider and the pavement (Henry, 2000). Because the slip speed of the BPT is very low, it is mainly dependent on micro-texture and is used as a surrogate for micro-texture (Henry, 2000).

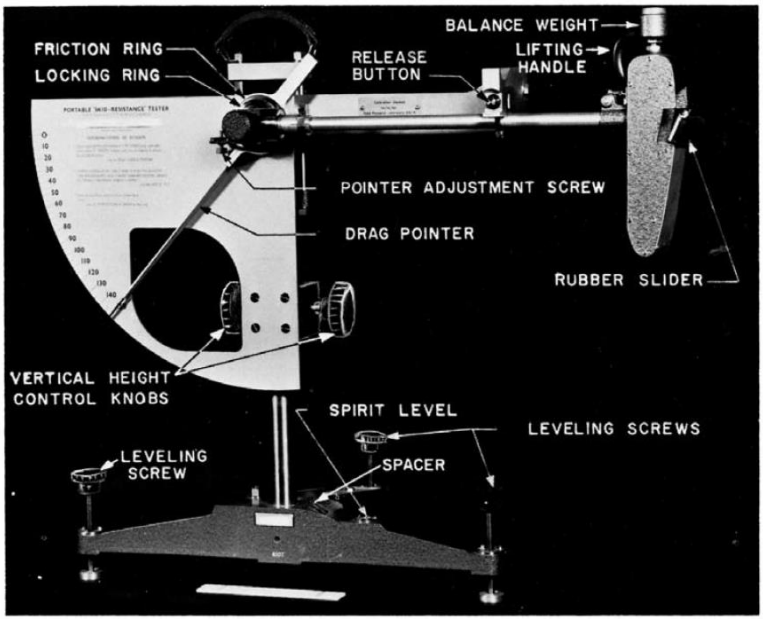

Figure 2 British Pendulum Tester (ASTM E3030-93, 2018)

Dynamic Friction Tester (DFT)

DFT (Figure 3) is a portable device measuring dynamic coefficient of friction (ASTM, 2018). A water supply unit delivers water to maintain a wet surface condition. The torque of the sliders is continuously measured during the testing for calculation of friction coefficients at various speeds in a single test run.

Figure 3 Dynamic Friction Tester

High-Speed Friction Measurements

The high-speed equipment can be subcategorized into four groups: locked-wheel (longitudinal friction force), side-force (sideway "lateral" friction factor), variable-slip, and fixed-slip (longitudinal friction force) (Hall et al., 2009). The last three devices can be characterized as continuous friction measurement equipment (CFME) because they conduct friction measurements continuously, greatly enhancing the ability to detect isolated low friction areas on pavements (de Leon Izeppi et al., 2016). More agencies around the world have started using CFME for highway friction management.

Locked-wheel Skid Tester

In the U.S., most state DOTs employ the locked-wheel skid tester, following ASTM E274 (2015), which simulates emergency braking without anti-lock brakes. The locked-wheel skid tester, as shown in Figure 4, is a trailer (of constant load and operated at a constant speed of 40 to 60 mph (65 to 100km/h) that hitches onto the back of a vehicle, and consists of two full-scale wheels, one of which is used for measuring (ASTM E274, 2015). The test wheel is equipped with either a standard ribbed-tire (ASTM E501) or a standard smooth-tire (ASTM E524). It is found that friction measurements with ribbed tire depend largely on the micro-texture, while friction measurement with smooth tire is sensitive to both the micro-texture and macro-texture (Li et al., 2004).

When a locked-wheel skid tester is in operation, an apparatus in front of the test wheel sprays water on the pavement to simulate a wetted surface condition. The test wheel is fully locked and produces 100 percent slip condition for friction measurement. It measures the coefficient of friction every one to three seconds and report the averaged value called Skid Number (SN) (ASTM E274, 2015).

Figure 4 Locked-wheel Skid Tester

Continuously Friction Measurement Equipment (CFME)

CFMEs have the advantage that they continuously measure the friction across the entire stretch of a road, providing greater detail about spatial variability of the tire pavement frictional properties (Flintsch et al. 2012), using either side-force or fixed-slip device.

Side-force Device

The side-force method measures the ability of vehicles to maintain control in curves with the angled wheel. The yaw angle between the tire and the direction of motion is typically small, between 7.5 to 20° (Hall et al., 2009). The small yaw-angle combined with low slip-speeds results in sensitivity to micro-texture, but often an insensitivity to macro-texture (Hall et al., 2009). Mu-Meter (ASTM E670, 2015) and Side-Force Coefficient Road Inventory Machine (SCRIM) are the two most common side-force devices. SCRIM was developed in 1960s in the UK and currently used in Australia, throughout Europe and in some parts of Asia (Austroads, 2011). The side-force measuring device can continuously monitor skid resistance on a network scale.

Variable-slip Device

The associated standard of the variable-slip device is ASTM E1859. This equipment utilizes a test wheel, capable of measuring longitudinal friction with a full range of speeds, from free rolling to fully lock. During operation, this equipment works by reducing the free-rolling velocity of the test wheel until it achieves a fully-locked condition, while simultaneously recording the frictional

forces as the tire progresses through the range of percent slip (0 to 100) (Hall et al., 2009). An example of variable-slip equipment is the Road Analyser and Recorder (ROAR), which is a compact unit with a single test wheel and able to mounted to a host vehicle. It can operate in either fixed or variable slip modes. Compared with other testers, it has the advantage of measuring the coefficient of friction at varying slip ratios in a single test run (Austroads, 2011).

Fixed-slip Device

The fixed-slip device (Figure 5) measures the rotational resistance at a constant slip speed (12 to 20 percent) (Hall et al., 2009). A widely used fixed-slip device is Grip Tester (Figure 5), which consists of a trailer that hitches onto the back of a vehicle, and operated under a constant load and at a constant speed of 40 to 60 mph (ASTM, E2340/E2340M-11, 2015). The fixed-slip device provides the coefficient of friction continuously, rather than periodically locking up and measuring skid resistance. Friction is measured by a single testing wheel at a steady test speed and reported as FN at 1m (3.28ft) interval.

Figure 5 Grip Tester

Factors Influencing Friction Measurements

According to NCHRP (Hall et al., 2009), the factors that influence pavement friction forces can be grouped into four categories: pavement surface characteristics, vehicle operational parameters,

tire properties, and environmental factors. Specifically, various factors are reviewed in the following sub-sections, including pavement surface texture; pavement condition; slip speed; water film depth; temperature; road geometry, et al.

Pavement Surface Texture

Pavement micro- and macro-texture are the main pavement surface characteristics that affect tire-pavement friction. Micro-texture (< 0.5mm depth) is the dominant factor in determining wet skid resistance at low to moderate speeds. Micro-texture is still important at high speeds but the macro-texture (0.5mm to 50.0mm) becomes dominant, as it provides rapid drainage routes between the tire and road surface (VicRoads, 2018).

Mean profile depth (MPD) and mean texture depth (MTD) are among the mostly used texture parameters, whose relationships to pavement friction are widely studied but not consistent among the studies (Hall et al., 2008; Kargah-Ostadi et al., 2015).

Macro-texture can be controlled by pavement treatments. Some typical macro-texture depths of different treatments are summarized in Table 2 (Merritt et al., 2015). Although there is no codified typical friction value for a given treatment, many studies were conducted to investigate the properties of different treatments. It was found by Li et al. (2012) that the friction of microsurfacing surface increased significantly in the first six months and reached the maximum number approximately after 12 months of service; UTBWC is capable of providing sufficient and consistent skidding resistance to allow quick opening to traffic. Several studies (de Leon Izeppi et al., 2010; Bledsoe 2015) claimed that High Friction Surface (HFS) can provide significant increase on surface skid resistance with a positive economic benefit. Li et al. (2007) compared friction performance of coarse aggregate and Hot-Mix asphalt pavements, and concluded coarse aggregate pavement (such as open-graded friction course (OGFC) and stone mastic asphalt mix) generated more consistent friction performance than other regular mixes.

Table 2 Typical Macro-Texture Depth for Various Pavement Treatments (Merritt, Lyon, and Persaud, 2015)

Pavement Treatment	Typical Macrotextue Depth
Slurry Seal	0.3 to 0.6 mm
Thin Hot Mix Asphalt Overlay	0.4 to 0.6 mm (Dense Graded) >1.0mm (Stone Matrix Asphalt)
Microsurfacing	0.5 to 1.0 mm
Diamond Grinding	0.7 to 1.2 mm
Grooving	0.9 to 1.4 mm
Ultra-Thin Bonded Wearing Course (UTBWC)	>1.0 mm
Chip Seal (various binder types)	>1.0 mm
Open Graded Friction Course (OGFC)	1.5 to 3.0 mm
High Friction Surfacing (HFS)	>1.5 mm

Pavement Condition

Pavement condition indices, such as International Roughness Index (IRI) and rutting, can undermine pavement drainage performance and vehicle stability which could reduce the skid resistance between vehicles and pavements (Arhin et al., 2015; Fwa et al., 2016).

Slip Speed

The coefficient of friction between a tire and the pavement changes with varying slip, which is expressed as the percentage of the ratio of slip speed to vehicle velocity. As illustrated in Figure 6, which is increasing rapidly to a peak value usually at 10 to 20 percent slip and then decreases to a value known as the coefficient of sliding friction that occurs at full sliding (Hall et al., 2009).

In dry conditions the level of surface friction is considered to be constant with increasing vehicle speed. However, in wet conditions, the level of surface friction reduces rapidly with increasing vehicle speed (Vicroads, 2018).

Since it is very difficult to maintain a standard speed on open roadways, many studies explored methods to convert the skid resistance from one speed to any desired speed. Flintsch et al. (2010) conducted a study to quantify the relationship for locked-wheel skid tester between speed adjustment factor and MPD for smooth tire and ribbed tire measurement respectively.

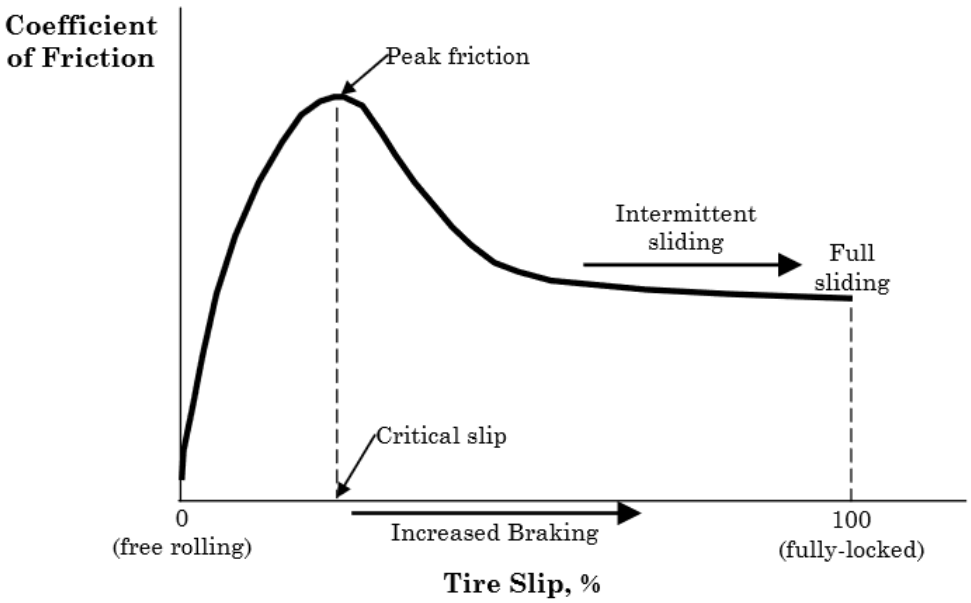

Figure 6 Coefficient of Friction versus the Percentage of Tire Slip (Hall et al., 2009)

Water Film Thickness

A study of NCHRP (2009) points out that water, can act as a lubricant, significantly reducing the friction between tire and pavement. The effect of water film thickness on friction is minimal at low speeds (<20mph or 32 km/h) and quite pronounced at higher speeds (>40mph or 64 km/h). In fact, a water film thickness of 0.002 inches reduces the tire pavement friction by 20 to 30 percent of the dry surface friction (Merritt et al., 2015).

Pavement macro-texture and tires threads can provide channels for water to escape through the tire pavement contact area which results in increasing the traction between tire and the pavement surface (Flintsch et al., 2012). It is known that worn tires are more sensitive to water film thickness. Ribbed tires are less sensitive to the operational test conditions and water film thickness. Some recommend ribbed tires as the preferred choice for friction measurement (Henry, 2000). However, ribbed tires are less sensitive to the pavement macro-texture, so it is recommended that their measurements be accompanied by macro-texture measurements (Flintsch et al., 2012).

Temperature

Research has indicated that the tire-pavement friction decreases if the tire temperature increases (Hall et al., 2009). Anupam et al. (2013) observed that higher temperature resulted in a lower hysteretic friction for a given pavement surface and a given tire slip ratio.

Bianchini et al. (2011) did a research on the temperature influence on the skid number of asphalt pavement surfaces when measured by the locked-wheel skid tester. The results showed that it was possible to define a reference temperature to adjust friction measured at any other temperature value. The reference temperature identified is between 19.5°C (67.1°F) and 20.2°C (68.4°F). The friction adjustment factors were ranged from -2, at approximately 4.4°C (40°F), to 2 for 32.2°C (90°F).

Road Geometry

Vicroads (2015) pointed out that the highest rates of loss to surface friction were found at sites where the highest vehicle stresses were imparted onto the surface aggregates, such as at tight curves and the approaches to intersections. At these sites, polishing of the surface aggregate occurs. It is also recognized that crossfall and superelevation will have effects on the propensity of water to pond on a road surface.

Pavement Skid Resistance and Highway Safety

Highway safety is a critical transportation issue in the United States. The first strategic goal in the FHWA Strategic Plan (2018) is focusing on safety: the use of a data-driven approach to reduce transportation-related fatalities and serious injuries across the transportation system.

Factors contributing to roadway crashes can be classified into three general categories (HSM, 2010):

- Human (driver and/or passenger behavior)

- Vehicle (design and condition)
- Roadway environment (design and condition)

At the era of autonomous driving and connected vehicles, the role of roadway on crashes will become more important. Factors in the roadway category include surface conditions (skid resistance, IRI, etc.) and roadway geometry (curves, grade, shoulders, etc.). Miller and Zoloshnja (2009) found that inadequate roadway condition is a contributing factor in more than half, 52.7 percent, of the nearly 42,000 American deaths resulting from motor vehicle crashes each year and 38 percent of the non-fatal injuries, resulting in more than $217 billion of economy loss each year. Many studies have consistently shown a link between crashes and roadway characteristics. The National Transportation Safety Board and FHWA found that about 70 percent of wet pavement crashes could be prevented or minimized by improved pavement friction (FHWA, 2016). A comprehensive relationship between friction and crash rate was found by Wallman and Astrom (2001) and revealed that the higher friction can significantly reduce the crash rate (Table 3):

Table 3 Relationship between Friction Coefficient and Crash Rate (Wallman and Astrom, 2001)

Frictional Coefficient	*Crash Rate (injuries per million vehicle km)*
<0.15	0.80
0.15-0.24	0.55
0.25-0.34	0.25
0.35-0.44	0.20

The AASHTO Highway Safety Manual (HSM, 2010) provides an approach that utilizes regression equations, the Safety Performance Functions (SPFs), to predict the crash frequency for a specific site type. Although roadway condition is listed as one category of contributing factors of crash, it is not fully considered in the current SPFs. The SPFs for highway segments in AASHTO HSM are functions of annual average daily traffic (AADT) and the segment length, which are both crash exposure indicators (HSM, 2010). Highway agencies are encouraged to develop state-specific SPFs for different roadway facilities and crash types (Merritt, et al., 2015).

For example, the SPF in Virginia is developed to include skid resistance and the radius of curvature for interstate and primary highway system (de León Izeppi, et al., 2016).

The jurisdiction-specific SPFs are likely to enhance the reliability of the Part C predictive method (HSM, page A-9, 2010; Lu et al., 2012). According to FHWA-SA-14-004 report, the steps in developing SPFs include (Srinivasan, Carter, and Karin Bauer, 2013):

> Step 1- Identify Facility Type. Depending on whether the SPF is being estimated for project-level analysis or network screening, the jurisdiction can decide which facility types they are most interested in.
>
> Step 2 - Compile Necessary Data. Depending on whether the SPFs will be used for project level analysis or network screening, the data needs are quite different.
>
> Step 3 - Determine Functional Form. The SPFs in Part C of the HSM and in Safety Analyst are negative binomial regression models with a log-linear relationship between crash frequency and site characteristics.
>
> Step 4 - Develop the SPF. A number of statistical tools (statistical software) are available to develop SPFs. Common ones include SAS, STATA, and GENSTAT (all commercially available software packages). Other software, including R, an open source programming language, and Microsoft Excel, can be used as well.
>
> Step 5 - Conduct Model Diagnostics. These include checking the sign of the parameters' coefficients, examining residuals via residual plots and cumulative residual plots (i.e., CURE plots), and identifying potential outliers using Cook's D or other tools, and examining goodness-of-fit measures.

Step 6 - Re-estimate the SPF. Based on the results of Step 5, the SPF may have to be re-estimated using a different statistical model or functional form. The SPF may also need to be re-estimated after removing outliers that were identified in the diagnostics step.

Furthermore, the statistically reliability of average crash estimation can be improved by combining observed crash frequency and estimates of the average crash frequency, using the Empirical Bayes predictive method (EB Method) to compensate for the potential bias resulting from regression-to-the-mean (RTM). The RTM is the tendency of crash fluctuations where a comparatively high crash frequency is followed by a low crash frequency (Hauer, 1996). Failure to account for the RTM bias may result in an over- or under- estimation of long-term crash frequency. The Empirical Bayes (EB) method is commonly known to address two problems of safety estimation: it increases the precision of estimates beyond what is possible when one is limited to the use of two-three years of history accidents, and it corrects for the RTM bias. The EB method uses a weighted adjustment factor, w, which is a function of the SPF's over-dispersion parameter, k, in the negative binomial distribution:

$$w = 1/(1 + k \times (\sum_{all\ study\ years} N_{predicted})) \qquad (2)$$

Therefore, the expected average crash frequency for the analyzed period is:

$$N_{expected} = w \times N_{predicted} + (1 - w) \times N_{observed} \qquad (3)$$

CHAPTER III

EVALUATION OF GRIP TESTER BASED CONTINUOUS FRICTION MEASUERMENT EQUIPMENT (CFME)

CFME is recommended as an appropriate method for Pavement Friction Management (PFM) program (FHWA, 2010). This chapter is to evaluate the performance of CFME in two aspects: the repeatability and the influence of operational characteristics on CFME measurements. The evaluation will assist state DOTs and highway agencies in better understanding the implementation of CFME for friction measurements. In particular, the Grip Tester, one type of CFMEs, was utilized as the primary field friction data collection device.

Repeatability of Grip Tester Measurements

The repeatability, also known as precision, of any measuring device is a primary concern of equipment users. It is desired that continuous friction measurements are not altered from repeating runs taken with the same equipment under unchanged conditions. If the system is repeatable, the measurement error can be mapped and compensated for. If the measurements differ greatly, one can argue that the findings derived from the measurements are inaccurate. However, continuous friction measurements may differ to a certain degree from multiple runs due to the potential vehicle wandering or the performance of the friction tester. As a result, it is necessary to evaluate the repeatability of CFME measurements, and herein a Grip Tester is used for field data collection.

Friction measurements can be affected by many factors, such as pavement surface type, testing

speed, water film thickness, tire characteristics, temperature and so on (AASHTO, 2008). To fully investigate the repeatability of Grip Tester measurements, testing sites with various pavement preventive treatments should be included for both concrete and asphalt pavements. For each site, multiple repeating runs were performed by the Grip Tester, owned by OSU, under the same operational conditions (0.25mm water film depth and 40mph vehicle speed). Five testing sites were selected and tested over the course of two field trips. Three of them were tested in November 2018: Lakeview Road in Stillwater (flexible pavement with Micro-surface), SH-33 in Perkins (concrete pavement with longitudinal grooving), and US-77 North Bound in Norman (concrete pavement with five types of preventive treatments including shotblasting). The additional two testing sites were tested in March 2019: I-40 in Oklahoma City (high friction surface with lead in and lead out asphalt pavement) and US-177 in Ponca City (ultra-thin bounded wearing course (UTBWC) asphalt). The temperature impact of each site is neglected. The friction profile of each site is displayed in Figure 7.

Various methodologies are available for repeatability testing. Traditionally, repeatability is often reported in terms of standard deviation, which measures the variation of measurements taken by a single device under the same conditions. This approach involves calculating the variances for friction records at the same location of multiple repeated runs. The standard deviation of the variances can be obtained subsequently. Table 4 summaries the average friction numbers and standard deviations of the variances for multiple repeating runs on each site. It is found that the Grip Tester friction measurements are more repeatable on the longitudinal groove site and UTBWC site, whose standard deviations are 0.0004 and 0.0006 respectively.

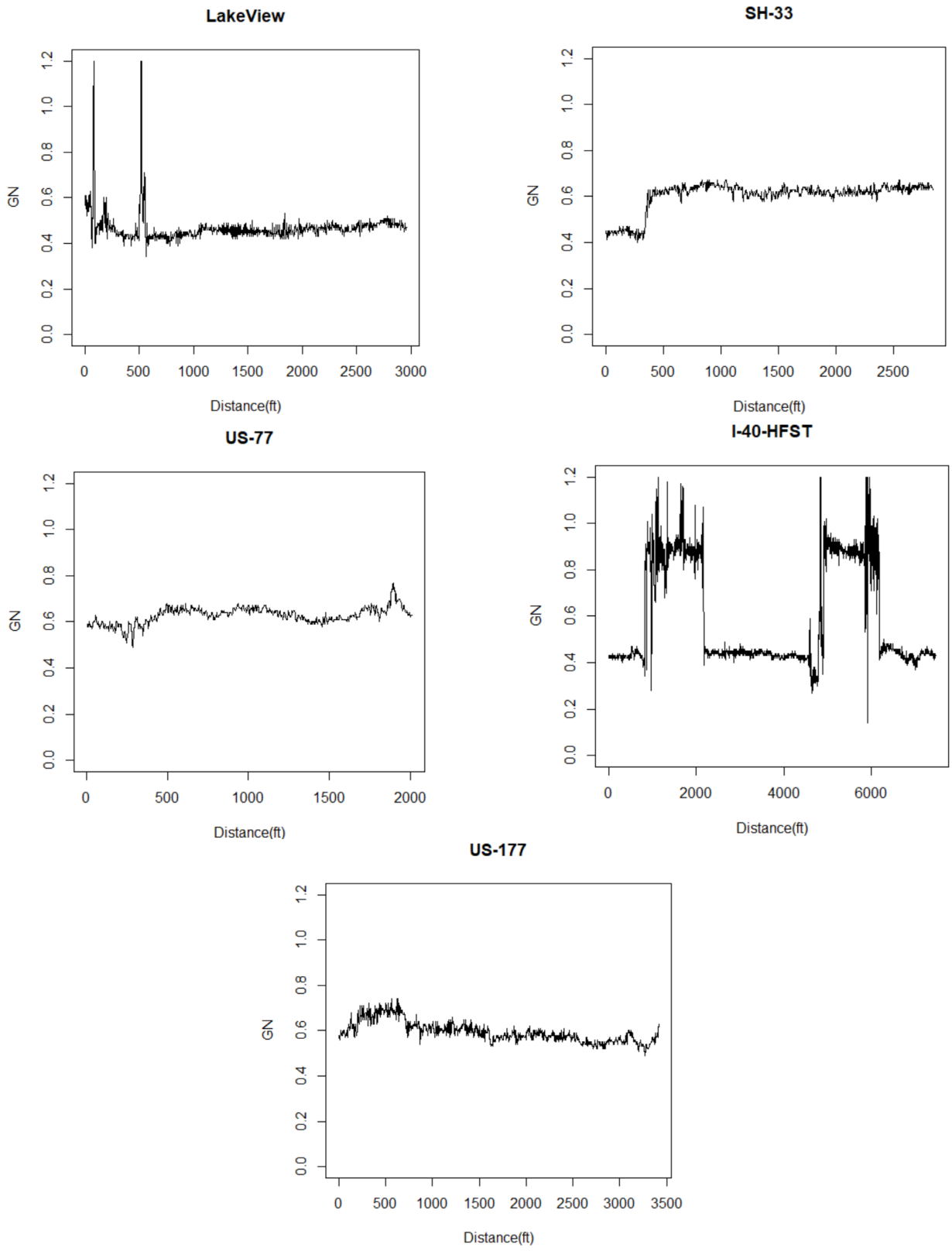

Figure 7 Grip Tester Friction Measurements

Table 4 Means and Standard Deviations for Evaluation of Repeatability

Site	Description	# of Run	1	2	3	4	5
Lakeview Rd	Micro-surface	Average FN	0.468	0.470	0.479	0.500	0.474
		Standard Deviation			0.0107		
SH-33	Longitudinal Groove	Average FN	0.604	0.612	0.625	0.615	0.630
		Standard Deviation			0.0004		
US-77-NB-R	Shotblasting	Average FN	0.628	0.586	0.602	0.565	/
		Standard Deviation			0.0012		
I-40-HFST	Asphalt & High Friction Surface	Average FN	0.591	0.619	0.652	0.645	0.653
		Standard Deviation			0.0125		
US-177	Ultra-thin Bonded Wearing Course	Average FN	0.595	0.596	0.592	0.604	0.602
		Standard Deviation			0.0006		

In addition, cross-correlation is a more rigorous statistical metric to identify the similarity among repeating measurements, which has been applied successfully in many disciplines, including pavement engineering in the areas of pavement longitudinal profiles (Karamihas, 2004) and friction profiles (Najafi et al., 2017) for repeatability and accuracy testing. The output of this methodology yields a single value, the cross-correlation coefficient, whose range is -1.0 to 1.0, whereby 1.0 indicates a perfect positive correlation, and -1.0 indicates a perfect negative correlation.

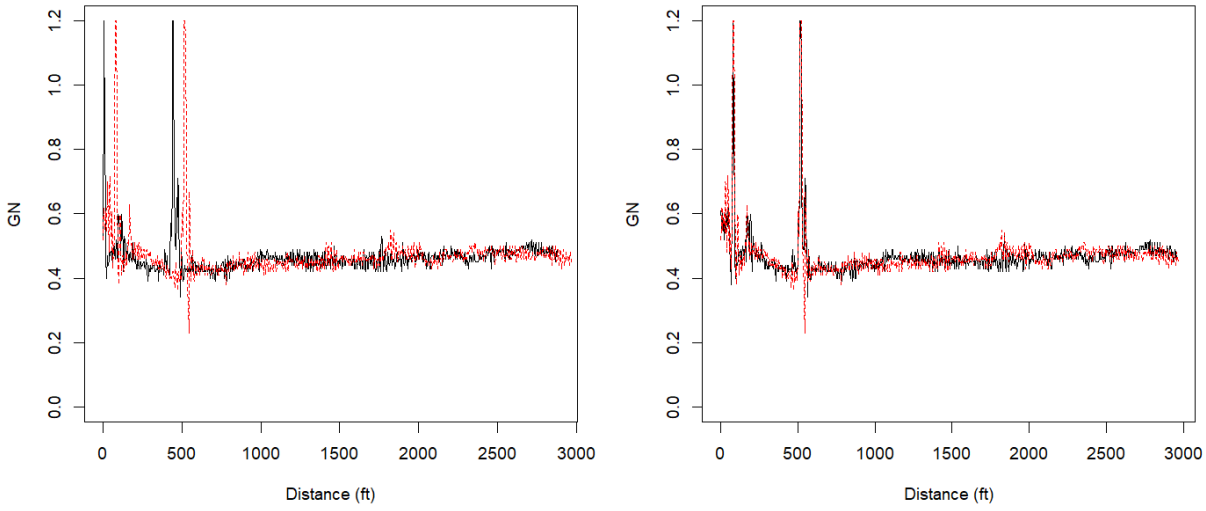

(a) Correlation at 0 Lag (b) Correlation at 22 Lags

Figure 8 Cross-correlation Methodology

Cross-correlation may also be employed to determine how much one waveform should be shifted to obtain the best match with another waveform, i.e. the optimal synchronization. The two friction profiles measured on Lakeview Road in Stillwater are shown in Figure 8(a): the first run (black line) and the second run (dotted red line). The two profiles are shifted in waveform by approximately 20 to 50 lags. The cross-correlation method is able to determine the optimum amount of shifting that provides the highest cross-correlation coefficient. The calculation process was performed by R programming. The maximum cross-correlation coefficient is 0.833 after the second run (dotted red line) is shifted to the left by 22 lags, as exhibited in Figure 8(b).

Table 5 Maximum Cross-correlation Value for Evaluation Repeatability

Sites	# of Run	1	2	3	4	5
Lakeview (Micro-surface)	1	1.000	0.833	0.592	0.573	0.714
	2	/	1.000	0.676	0.569	0.725
	3	/	/	1.000	0.582	0.794
	4	/	/	/	1.000	0.644
	5	/	/	/	/	1.000
SH-33 (Longitudinal Groove)	1	1.000	0.916	0.912	0.939	0.925
	2	/	1.000	0.863	0.878	0.881
	3	/	/	1.000	0.902	0.878
	4	/	/	/	1.000	0.887
	5	/	/	/	/	1.000
US-77 (Shotblasting)	1	1.000	0.534	0.633	0.484	/
	2	/	1.000	0.782	0.735	/
	3	/	/	1.000	0.621	/
	4	/	/	/	1.000	/
I-40 (HFST& Asphalt)	1	1.000	0.955	0.926	0.943	0.943
	2	/	1.000	0.954	0.959	0.950
	3	/	/	1.000	0.941	0.950
	4	/	/	/	1.000	0.950
	5	/	/	/	/	1.000
US-177 (UTBWC)	1	1.000	0.817	0.828	0.662	0.838
	2	/	1.000	0.873	0.637	0.855
	3	/	/	1.000	0.688	0.871
	4	/	/	/	1.000	0.647
	5	/	/	/	/	1.000

Cross-correlation analysis is subsequently applied to the possible combinations of multiple runs, and the results for the five testing sites are shown in Table 5. The highest repeatability is obtained

on the HFST section, but there is relatively weaker repeatability on the shotblasting site. The friction profile of the shotblasting site is uniform in shape without distinct changes (Figure 7), which makes the synchronization process more challenging. For the HFST site, since there is a significant increase of friction from the non-HFST to HFST surface, the synchronization of the measurements is easier and more accurate. Additionally, the wandering of the testing vehicle during measurements could reduce the correlation among different runs. Overall, the results suggest that the Grip Tester based CFME measurements have sufficient repeatability.

Influence of Operational Characteristics on Grip Tester Measurements

Understanding the influence of various factors on CFME measurements has many benefits in guiding state agencies to effectively implement CFME for the PFM. The influencing factors for pavement friction measurements can be put into four categories: pavement surface characteristics, vehicle operational parameters, tire properties, and environmental factors (AASHTO, 2008; Austroads, 2009). Most previous studies (Hall et al., 2009; Vicroads, 2018; Flintsch et al., 2010) only investigated limited number of influencing factors while other characteristics were held as constants. This section aims to investigate and quantify the influence of various characteristics on Grip Tester based CFME measurements via a comprehensive field data collection and statistical multiple regression analysis.

The influencing factors investigated in this study include pavement texture parameters, pavement conditions in terms of IRI, temperature, vehicle speed, and water film depth during the testing. To better quantify pavement surface texture, instead of the commonly used texture indicator mean profile depth (MPD), a novel signal processing technique, Hilbert-Huang Transformation (HHT), is implemented to extract amplitude and instantaneous frequency information as the potential texture parameters. This process will be discussed later in detail.

Field Data Collection and Preprocessing

In order to investigate the effects of various characteristics on the continuous friction measurements, 22 testing sites were selected as the testing bed in the State of Oklahoma, including:

- Ten types of preventive maintenance treatments: chip seal, ultra-thin bounded wearing course (UTBWC), asphalt resurface, warm mix asphalt, microsurface, high friction surface treatment (HFST), concrete resurface, longitudinal grooving, next generation concrete surface (NGCS), and shotblasting.
- Nine combinations of friction testing conditions: three water film depths (0.25, 0.50, 1.00mm) combined with three different testing speeds (40, 50, 60mph for major arterials, while 30, 40, 50mph for minor arterials).

The range of ambient temperature during testing was from 56 to 110°F. Field friction data was collected using the Grip Tester. The corresponding pavement texture data was acquired by an AMES 8300 Survey Pro High Speed Profiler. The Profiler is capable of collecting both macro-texture data and longitudinal profiles at highway speed at 0.25mm (0.00082ft) interval. The collected profile can be used to calculate mean profile depth (MPD) and the international roughness index (IRI).

For each testing scenario, a uniform 500ft-long pavement section was selected for analysis, and the corresponded IRI value, temperature during testing, testing speed, and water film depth are acquired.

Prior to extracting the texture characteristics, it is important to remove noises from the longitudinal pavement profiles (Katicha et al., 2015). One simple, but widely used, method is the use of the mean plus or minus three times of standard deviation for outlier detection. Statistically, approximately 0.26% of the data samples are identified as outliers (Howell, 1998). However, this

method is limited to the normal distribution, and its mean and standard deviation are strongly affected by the outliers. In this study, an alternative to this fixed threshold is used, the Median Absolute Deviation (MAD) from the median of a univariate data set. Subsequently, the Hampel filter (Salem et al., 2013) is applied using the MAD results as the outlier resistant parameters.

The first step of Hampel filtering is to obtain the median (∅) of a sliding window (Equation (4)). A window is composed of a point of interest and its N surrounding samples, with N/2 data points each side. Later, the MAD of the sliding window is calculated using Equation (5), which is the median of the set difference between each point and the ∅. An outlier is identified if it differs from the median by a threshold value related to the MAD (Equation (6)). Lastly, the detected outliers are replaced by the median of the sliding window (∅). This methodology is executed in R programming. One example is displayed in Figure 9. Figure 9(a) is the original texture profile. The outliers are detected as red dots in Figure 9(b), and the denoised profile is shown in Figure 9(c).

$$\emptyset = median(H_1, H_2, \dots H_N) \quad (4)$$

$$MAD = median(\,|H_i - \emptyset|) \quad (5)$$

$$|H_i - \emptyset| > k \times MAD \quad (6)$$

Where H is the relative depth of pavement texture, and k is the threshold value.

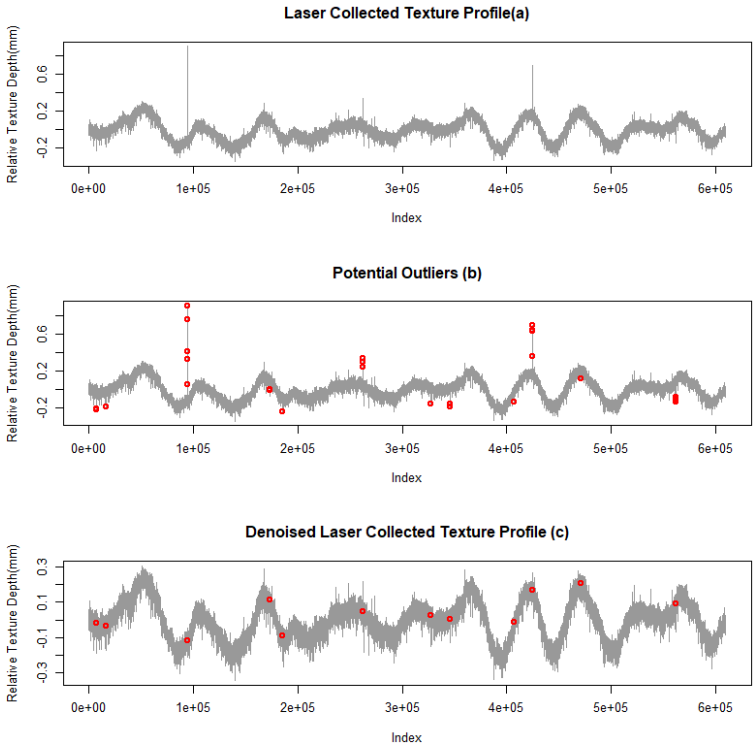

Figure 9 An Example Pavement Texture Profile: Original and After Denoising

Hilbert-Huang Transformation (HHT) Based Texture Profile Analysis

After removing noises from the texture profiles, the HHT technique is applied to extract the texture characteristics. HHT is an adaptive methodology based on the local characteristic in the time scale of the data and is, thus, suitable for analyzing non-linear and non-stationary signals (Huang et al., 1998; Kane and Rado, 2015; Rado and Kane, 2014). The obtained texture information from the HHT process is deployed as the influencing factors to represent the physical characteristics, such as sharpness and curvature of the texture asperities (Cho et al., 2010). The HHT technique consists of two major processes: the empirical mode decomposition (EMD) and the Hilbert spectral analysis (Huang et al., 1998).

Empirical Mode Decomposition (EMD)

Each denoised pavement texture profile is decomposed, according to the EMD process, into a set of basic profiles, called as the Intrinsic Mode Function (IMF) (Gagarin, 2014), C_j:

$$H(x) = r_n(x) + \sum_{j=1}^{n} C_j(x) \quad (7)$$

Where H is the relative depth of a pavement profile at distance (or time) x; n is the total number of IMFs; r_n is the residue of the decomposition, which can be either termed as a monotonic function or a constant.

Each IMF represents a simple oscillatory mode, which can be linear or non-linear based upon the characteristics of the data (Huang et al., 1998). To extract the IMFs, the EMD consists of the following steps. First, construct upper envelope by connecting all the local extrema with a cubic spline line. Second, repeat the procedure to produce the lower envelope. The upper and lower envelopes should cover all the data between them. Third, their mean is computed and subtracted from the original data. The result is the first candidate IMF. This sifting process can be repeated until the resulting function satisfies the definition of IMF (Huang, 1998):

- the number of local maxima and the number of local minima differs at most by one;
- the upper and lower envelopes of the signal are symmetric with respect to zero.

Figure 10 illustrates an example pavement texture profile and its EMD results. Each IMF has a mean of zero. The component with highest frequency is extracted as the first IMF (IMF1), and the remaining signal is considered as the residue of IMF1. Subsequently, the second IMF (IMF2) is obtained by taking the residue signal as a new signal and repeating the EMD process. The sifting process can be stopped when the residue becomes a monotonic function or a constant, which is usually an indicative trend of the original data (Huang, 1998; Ayenu-Prah and Attoh-Okine, 2009). In this study, each texture profile was decomposed to a maximum of 10 IMFs.

The obtained IMFs represent the actual sharpness, power, and curvature of the texture asperities at different scale classes, which could relate to the frictional characteristics of pavement surfaces (Rado and Kane, 2014).

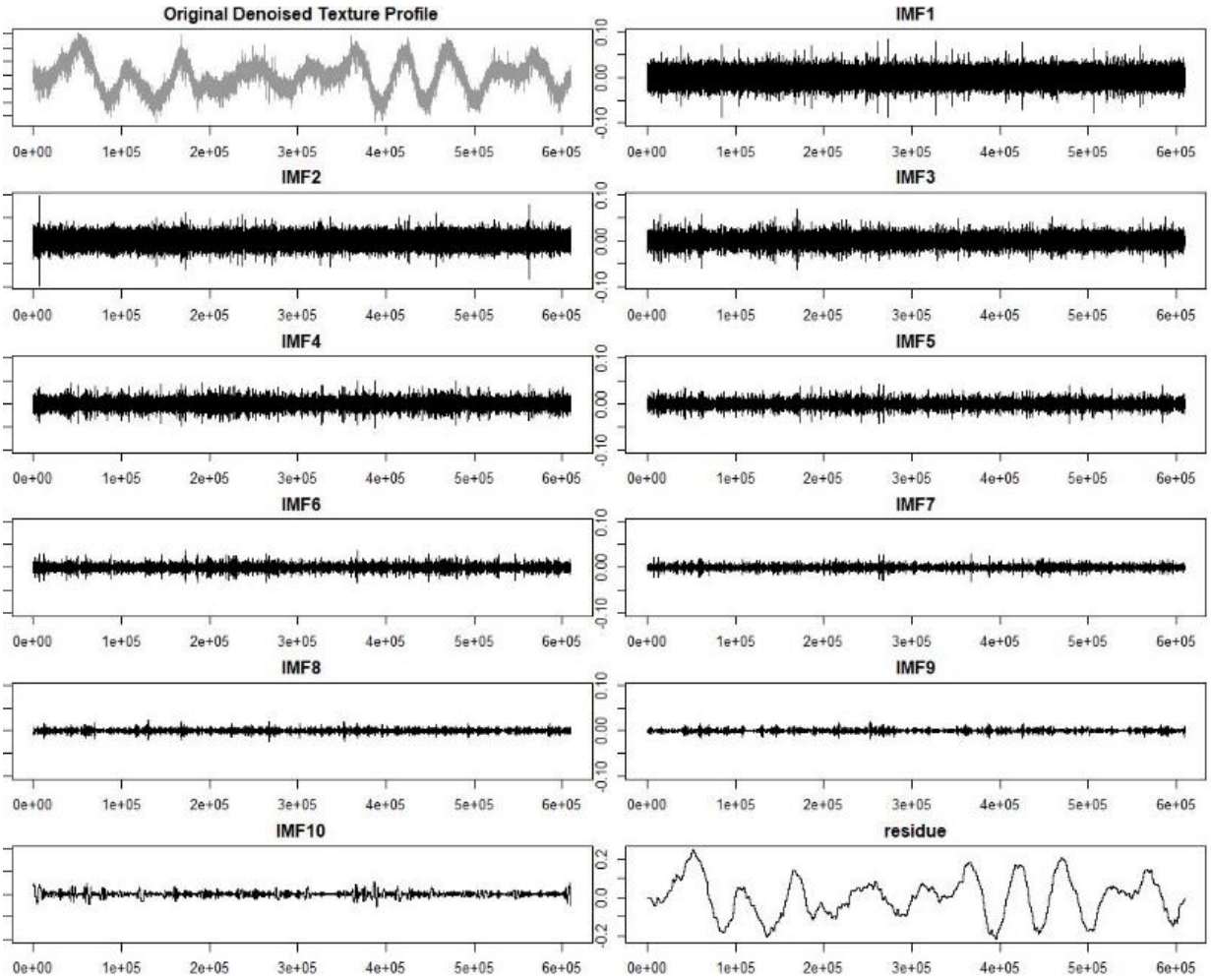

Figure 10 An Example of An Original Pavement Profile and Its Decomposed IMFs and Residue

Hilbert Spectral Analysis

After the EMD process, the Hilbert spectral analysis is performed on each IMF component to compute the instantaneous frequency as the derivative of the phase function and then extract the localized texture information. The results of Hilbert spectral analysis can subsequently yield a full energy-frequency-time distribution of the signal in the Hilbert spectrum (Ayenu-Prah and Attoh-Okine, 2009). Thereby, the original data can be expressed as the real part, Re, in the following form (Gagarin, 2014):

$$H(x) = Re\ \sum_{j=1}^{n} a_j\,(x) e^{i\int \omega_j(x)dx} \qquad (8)$$

Where, $a(x)$ and $\omega(x)$ represent the amplitude and instantaneous frequency as a function of distance (or time) variable x.

Subsequently, the amplitude (A_i) and instantaneous frequency (F_i) of the ith IMF_i are averaged into texture parameters, which are further used to investigate their influences on pavement friction measurements.

Statistical Analysis and Results

A multiple regression analysis is conducted to quantify the effects of different characteristics on the continuous friction measurements. The influencing factors include the texture parameters from the HHT process, IRI, temperature, Grip Tester testing speed and its water film depth. The multiple regression model is expressed in the formula below:

$$Friction\ Number = \varphi + \sum_1^n \alpha_i * X_i \quad (9)$$

Where, φ is the estimated intercept; X_i represents the influential parameters; α_i is the estimated coefficient of corresponding parameters.

Backward stepwise regression is applied to develop the final multiple regression model. It starts with all the variables included in this study, then gradually removes the least significant variable at each step and finds a reduced model that best explains the data. The statistical results of the multiple regression analysis are displayed in Table 6.

Average IRI, temperature, testing speed, water film depth, and a portion of the texture parameters are statistically significant for the friction measurements at more than 99.99% level of confident. The adjusted R-squared is 0.88 and the p-value of the model is less than 0.05, indicating that the model is significant. Temperature, testing speed, and water film depth show negative effects on the friction measurements. That is, the increases of these operational characteristics will result in decreases of measured friction numbers. These findings are consistent with those from several previous studies (Hall et al., 2009; Vicroads, 2018). Average IRI is found to have a positive effect on friction measurements. It is logical since the bouncing of the Grip Tester on rough surfaces may result in an increase of the dragging force (F) and a decrease of the force (N) perpendicular

to the pavement surface. As a result, the coefficient of friction, which is the ratio of F over N, increases. It is also noted the Grip Tester friction measurement is more sensitive to the change of water film depth and some of the texture parameters. However, the effects of some texture parameters on friction data are positive, while others are negative. Although these parameters from the HHT process are believed to reflect the actual sharpness, power, and curvature of the texture asperities at different scale levels; thus far, no consistent conclusions are available to explain their detailed physical meaning. Further research is, therefore, needed to explore the physical meanings of these parameters and the mechanism on why they matter.

Table 6 Multiple Regression Results

Parameters	Coefficients	Std. Error	t value	Pr(>|t|)	Significant Level
(Intercept)	-4.84E-01	1.70E-01	-2.85	0.004883	**
Average IRI (in/mi)	2.19E-03	2.87E-04	7.641	1.21E-12	***
Temperature (F)	-4.59E-03	4.59E-04	-9.997	< 2e-16	***
Speed (mph)	-3.04E-03	4.61E-04	-6.599	4.43E-10	***
Water Film Depth (mm)	-1.01E-01	1.18E-02	-8.564	4.65E-15	***
F_2	2.81E-05	4.26E-06	6.591	4.62E-10	***
F_4	4.95E-05	5.89E-06	8.41	1.20E-14	***
F_6	-3.75E-05	8.67E-06	-4.326	2.51E-05	***
F_7	-3.67E-05	1.04E-05	-3.516	0.000554	***
F_8	3.77E-05	8.35E-06	4.517	1.13E-05	***
F_9	-1.99E-05	5.19E-06	-3.833	0.000175	***
F_{10}	1.50E-05	1.77E-06	8.505	6.67E-15	***
A_2	-6.80E+01	9.39E+00	-7.238	1.25E-11	***
A_3	1.73E+02	1.63E+01	10.607	< 2e-16	***
A_5	-8.02E+01	1.09E+01	-7.386	5.35E-12	***
A_7	-9.62E+01	8.95E+00	-10.749	< 2e-16	***
A_8	7.54E+01	6.29E+00	11.994	< 2e-16	***
	Signif. codes: 0 '***' 0.001 '**' 0.01 '*' 0.05 '.' 0.1 ' ' 1				
			Adjusted R-squared: 0.88		
			p-value: < 2.2e-16		

Utilizing the developed multiple regression model, the predicted and measured Grip Tester friction values are verified in Figure 11 with an adjusted R-squared of 0.88; this indicates the model could clearly demonstrate the response of the friction measurements of a Grip Tester. This

model may assist state agencies in better understanding the field friction measurements and prompting the implementations of CFMEs to support pavement friction management programs. In addition, this study also verifies the feasibility and usefulness of the HHT technique for the extraction of more meaningful pavement texture characteristics from pavement texture profiles, which could be correlate well to friction measurements.

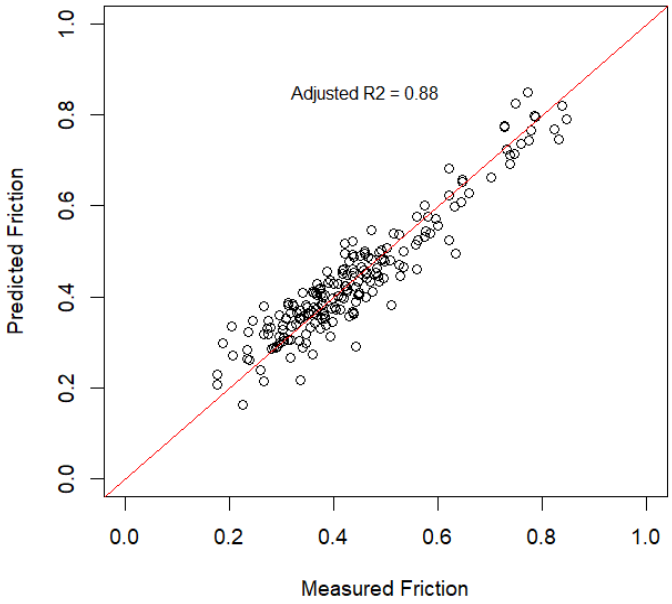

Figure 11 Predicted Friction versus Measured Friction

Conclusion

Through a comprehensive field data collection and analysis, the following conclusions can be drawn based on the results:

- The Grip Tester based CFME measurements have sufficient repeatability, which displays its capability to support the PFM program.
- HHT technique is feasible and useful for the extraction of meaningful pavement texture characteristics from pavement texture profiles, which correlate well to friction measurements.

- The Grip Tester measurement shows a negative response to the change of temperature, testing speed, and water film depth; whereas, it has a positive response to the change of IRI.
- The model developed using various operational factors and HHT indicators can be used to correct/adjust friction measurements conducted at different operation conditions for comparable results.

CHAPTER IV

RANDOM FOREST BASED PAVEMENT FRICTION PREDICTION USING HIGH RESOLUTION 3D IMAGE DATA

Many studies have concluded that pavement friction is dominated by the texture of pavement surface, especially the micro- and macro- texture characteristics. Many researchers have developed friction-texture models to explore the use of non-contact measurements for skid resistance evaluation, which could compensate for the limitations of current contact-based measurements, such as water consumption and subjecting to change with many operational factors. The objective of this chapter is to develop a friction prediction model using high resolution 3D texture data of pavement surfaces.

Currently, pavement surface texture is primarily measured at the macro-texture scale. Mean profile depth (MPD) and mean texture depth (MTD) are among the mostly used texture parameters, whose relationships to pavement friction are widely studied but not consistent among the studies (Flintsch et al., 2012; Hall et al., 2008; Kargah-Ostadi et al., 2015). With the advancement of non-contact high resolution 3D laser technology, it is becoming feasible to characterize pavement or aggregate surface texture at both macro- and micro- scales (Kargah-Ostadi et al. 2015; Kanafi et al. 2015; Li et al. 2012; Masad, 2005; Qian et al. 2017; Zuniga-Garcia, 2016), and investigate their influences on surface friction characteristics under traffic polish over time based on field data sets. In addition, incorporating texture at both macro- and micro- scales can improve the accuracy of friction prediction (Ergun et al., 2005; Serigos et al.,

2014; Chen et al., 2019).

Various texture parameters in disciplines other than pavement engineering are available for surface texture characterization and evaluation. In this chapter, the collected 3D high resolution pavement surface texture data was filtered into micro- and macro scales with twenty-seven 3D areal texture parameters including height parameters, volume parameters, hybrid parameters, spatial parameters, and feature parameters. Furthermore, these 3D areal texture parameters were correlated to the pavement friction using the random forest algorithm, one of the most popular machine learning technologies.

Field Data Collection

The field testing bed of this study was constructed in November 2015 by the Oklahoma Department of Transportation (ODOT), as a part of the LTPP SPS-10 project. Six warm mix asphalt (WMA) sections were constructed in this site, with the length of 500 ft for each section. Sections 1 to 3 are the LTPP required SPS-10 experimental designs, while sections 4 to 6 are supplemental sections with mixes chosen by the ODOT Division Office. The detailed mixture design information of each section is displayed in Table 7 (Yang et al., 2017). Three data collection trips were made in November 2015 (immediately after construction), June 2016 and January 2017. During each trip, 36 pairs of pavement friction and texture data were collected on predefined locations: three pairs on each section and three pairs on each transition section. In total, 108 pairs of pavement friction and texture data were collected in this study for data analysis.

Table 7 Experiment Design for LTPP SPS-10 Site in Oklahoma (Yang et al., 2017)

Section ID	Binder	Comment	Aggregate Combination	Insoluble Residue (%)
1	PG 70-28	HMA with RAP + RAS	1	56.3
2	PG 70-28	WMA Foaming with RAP + RAS	1	56.3
3	PG 70-28	WMA Chemical with RAP + RAS	1	56.3
4	PG 64-22	WMA Chemical with RAP + RAS	1	56.3
5	PG 58-28	WMA Chemical with RAP + RAS	1	56.3
6	PG70-28	WMA Stone mix with mineral filler	2	43.6
Mainline	PG70-28	HMA with RAP	3	60.8

Note:
Aggregate Combination 1 contains 38% 5/8 Chips + 35% Stone Sand + 12% Sand + 12% RAP + 3% RAS;
Aggregate Combination 2 contains 90% 5/8 Chips + 10 Mineral Filler;
Aggregate Combination 3 contains 34% 5/8 Chips + 13% Scrns. + 30% Stone Sand + 13% Sand + 10% RAP.

Pavement surface texture data was collected using the LS-40 scanner (Figure 12(a)). The 3D laser triangulation imaging technology is used in LS-40 to collect and process 2D/3D images: a built-in motor stage moves a very fine laser beam over target surface or objects; a high resolution camera takes laser beam images from an angle. The LS-40 scans a 4.5” by 4” pavement surface with height resolution (z) at 0.01mm and lateral resolution (x, y) at 0.05mm. Therefore, the obtained high resolution 3D surface image includes both pavement macro- and micro- texture characteristics.

Immediately after the LS-40 testing, a DFT (Figure 12(b)) was utilized to collect pavement friction data at the same location. DFT is a portable device measuring dynamic coefficient of friction (ASTM E1911-09a, 2009). A water supply unit delivers water to maintain a wet surface condition. The torque of the sliders is continuously measured during the testing for calculation of friction coefficients at various speeds, from 10 km/h to 80 km/h.

(a) LS-40 Portable 3D Surface Analyzer

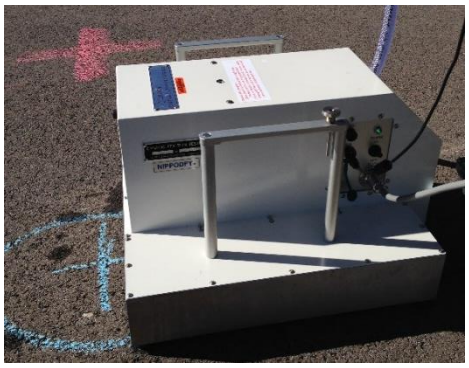

(b) Dynamic Friction Tester (DFT)

Figure 12 Data Collection Devices

Data Preprocessing Using Butterworth Filtering

Since the LS-40 texture data contains both macro- and micro-texture information, it is desired to separate the two components for the development of friction models. The Butterworth filter is a signal processing technique which passes or stops certain frequencies of interest. Zuniga-Garcia and Prozzi designed a Butterworth filter to isolate micro- and macro-texture wavelengths from field pavement surface data. As shown in Figure 13, a customized band pass Butterworth filter is designed in this study to separate macro- and micro-texture from the collected high-resolution 3D pavement images. In this filter, all the frequencies between 0.0008 and 0.08 cycles/m (wavelengths from 0.5 to 50 mm) are passed through for macro-texture, as shown in Figure 13(b), while the frequencies less than 0.08 cycles/m (wavelengths lower than 0.5 mm) are passed for the micro-texture information, as shown in Figure 13(c).

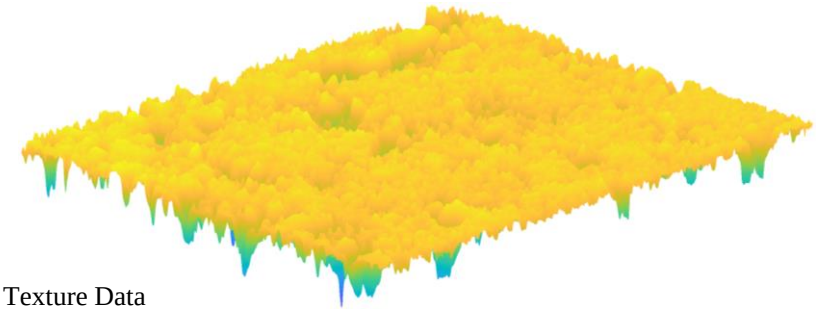

(a) Original 3D Texture Data

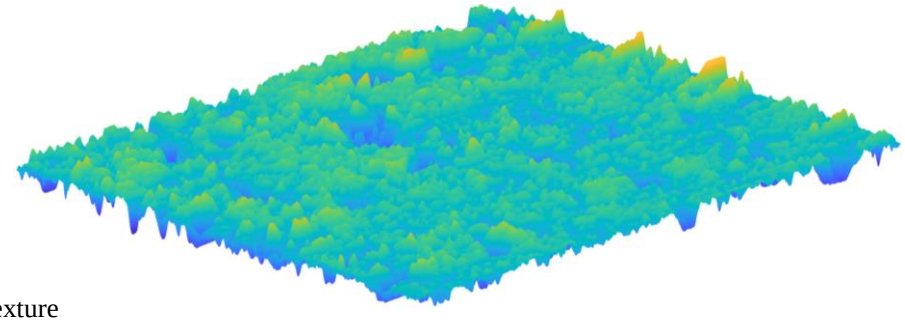

(b) Macro-Texture

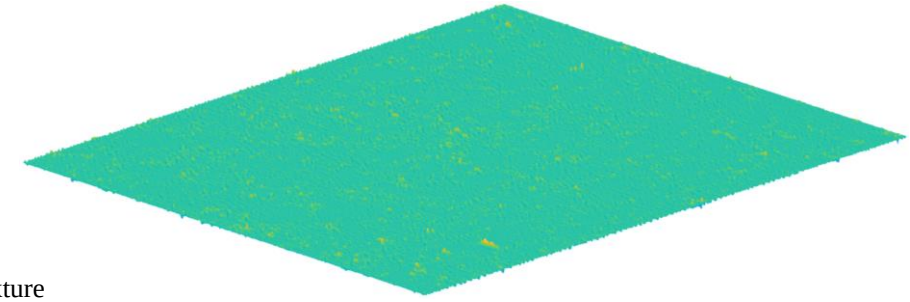

(c) Micro-Texture

Figure 13 Butterworth Filter

3D Areal Pavement Texture Parameters

Once the macro- and micro-texture data are separated from each 3D texture image, 3D areal texture parameters are calculated at both macro- and micro-scales. As shown in Table 8, twenty-seven 3D areal texture indicators are calculated in this paper, which can be categorized into five classes: seven height parameters, three spatial parameters, two hybrid parameters, six volume

parameters, and nine feature parameters. Due to the length limitations, the detailed definitions and equations of these texture parameters are omitted herein, which can be found in the ISO25178 standard (2012) and at Li et al. (2017).

Table 8 3D Areal Surface Texture Parameters

Categories	**ISO 25178 Parameters**	**Unit**	**Description**
Height	Sq	mm	Root mean square height of the surface
	Ssk	Unitless	Skewness of height distribution
	Sku	Unitless	Kurtosis of height distribution
	Sp	mm	Maximum height of peaks
	Sv	mm	Maximum height of valleys
	Sz	mm	Maximum height of the surface
	Sa	mm	Arithmetical mean height of the surface
Spatial	Sal	mm	Fastest decay auto-correlation rate
	Str	Unitless	Texture aspect ratio of the surface
	Std	-	Texture direction of the surface
Hybrid	Sdq	Unitless	Root mean square gradient of the surface
	Sdr	%	Developed area ratio
Volume (Functional)	Vm	mm^3/mm^2	Material volume at a given height
	Vv	mm^3/mm^2	Void volume at a given height
	Vmp	mm^3/mm^2	Material volume of peaks
	Vmc	mm^3/mm^2	Material volume of the core
	Vvc	mm^3/mm^2	Void volume of the core
	Vvv	mm^3/mm^2	Void volume of the valleys
Feature	Spd	$1/mm^2$	Density of peaks
	Spc	1/mm	Arithmetic mean peak curvature
	S10z	mm	10 point height
	S5p	mm	5 point peak height
	S5v	mm	5 point valley height
	Sda	mm^2	Closed dales area
	Sha	mm^2	Closed hills area
	Sdv	mm^3	Closed dales volume
	Shv	mm^3	Closed hills volume

Correlation Analysis of Friction Numbers

DFT friction numbers at 10, 15, 20, 25, 30, 40, 50, 60, and 70 km/h are selected herein to study the speed influence on friction performance. As discussed in the previous session, 108 DFT friction measurements are made from the three data collection events. The maximum friction number is 0.74, the minimum 0.19, and the median 0.38. Correlation analysis is subsequently conducted among the friction measurements at various speeds to identify the representative DFT friction numbers at both high and low speeds. In general, a correlation coefficient larger than 0.8 indicates a strong correlation while less than 0.5 indicates weak correlation. The correlation coefficients are summarized in Table 9.

As Table 9 shows, the friction numbers measured at 25 to 70 km/h and those measured at 10 to 20 km/h are highly correlated. Therefore, the friction numbers at 70 km/h and 15 km/h are selected to represent the high-speed and low-speed friction. Friction models at high and low speeds are subsequently developed with the aforementioned texture parameters.

Table 9 Correlation among DFT Friction Numbers at Different Speeds

	DFT70	DFT60	DFT50	DFT40	DFT30	DFT25	DFT20	DFT15	DFT10
DFT70	1.00								
DFT60	0.98	1.00							
DFT50	0.97	0.99	1.00						
DFT40	0.92	0.95	0.98	1.00					
DFT30	0.83	0.87	0.92	0.97	1.00				
DFT25	0.73	0.77	0.84	0.91	0.97	1.00			
DFT20	0.49	0.53	0.60	0.69	0.81	0.91	1.00		
DFT15	0.05	0.09	0.16	0.25	0.41	0.58	0.83	1.00	
DFT10	-0.20	-0.18	-0.13	-0.05	0.11	0.29	0.62	0.87	1.00

Implementation of Random Forest Algorithm

The random forest algorithm is a non-linear ensemble machine learning technique combining many decision trees to make a prediction for both classification and regression problems. For regression tasks, its main advantages are: i) the robustness regarding solve overfitting, ii) the comparatively small number of hyper parameters that have to be specified by users, iii) the

automatic computation of variable importance rankings that accesses the contribution of each variable to the final model, iv) the algorithm is very fast since training of each decision tree is independent (Hutengs et al., 2016).

In a random forest regression model, decision trees are paralleled and the mean prediction value is generated as the output of the model. The random forest can model the complex relationship between input variables and prediction other than detailed numerical expressions, with the following three steps (Fernández-Blanco et al., 2013):

- Obtain n random samples from the original dataset as tree seeds.
- For each seed grow a non-pruned tree, and for each node randomly choose m predictors and the best split among them.
- Execute the different prediction trees and select the most voted tree as the prediction.

Two key features of the random forest algorithm are out-of-bag (OOB) error estimates and variable importance rankings (Hutengs et al., 2016). In a random forest, each decision tree is trained via the bagging method, in which a subset data is randomly sampled with replacement from the original training set. With bagging, only approximately 63% of the training instances are sampled on average for each predictor, while the remaining 37% of the training instances that are not sampled are called OOB instances (Geron et al., 2017). The mean squared error (MSE) of the OOB samples is generally used to test error estimate, a similar measurement as k-fold cross-validation. Subsequently, every node in a decision tree in the forest is split into two, and the number of variables selected at each split is optimized by minimizing the OOB error of predictions (ISO, 2012). The algorithm records the decrease of weighted impurity at each split and each tree to evaluate the importance of a variable X_m for predicting Y (Breiman, 2001; Breiman, 2002), as shown Equation (1) known as Mean Decrease Impurity importance (MDI) (Louppe et al., 2013):

$$Imp\ (X_m) = \frac{1}{N_T} \sum_T \sum_{t \in T: v(S_t) = X_m} c(t) \Delta(S_t, t) \qquad (10)$$

Where N_T is the number of trees in the forest; $v(S_t)$ is the variable used in split S_t; c(t) is the proportion of samples reaching node t, calculated by N_t/N; $\Delta(S_t, t)$ represents impurity decreases for node t. In this regression task, the impurity decreases are evaluated by MSE. In Python programming, the importance of variable is normalized to a value between 0 and 1, refereed as the importance value in this study. The sum of the importance value in a random forest equals to one. The higher the importance value, the more important the variable X_m is for predicting Y.

To illustrate the process, Figure 14 displays an example decision tree randomly selected from the random forest (A suffix of "L" represents macro-texture; "S" represents micro-texture in all the figures in this chapter). The decision tree in Figure 14 is restricted to a depth of five for simplicity and demonstration. Each node displays four types of information: a binary condition; the value of MSE; number of samples reaching this node; prediction value of Y. As the tree grows, the number of samples is reducing until reaching to 1. Thereby, this decision tree gives a prediction for specific inputs. A final prediction is reached with most vote aggregated of all trees. For instance, if S_a at micro-scale is 0.5, S_{pc} at macro-scale is 5.0, and S_{td} at macro-scale is 95.0, the prediction of corresponding friction number is 0.2 based on this decision tree, as demonstrated by the dotted line in Figure 14.

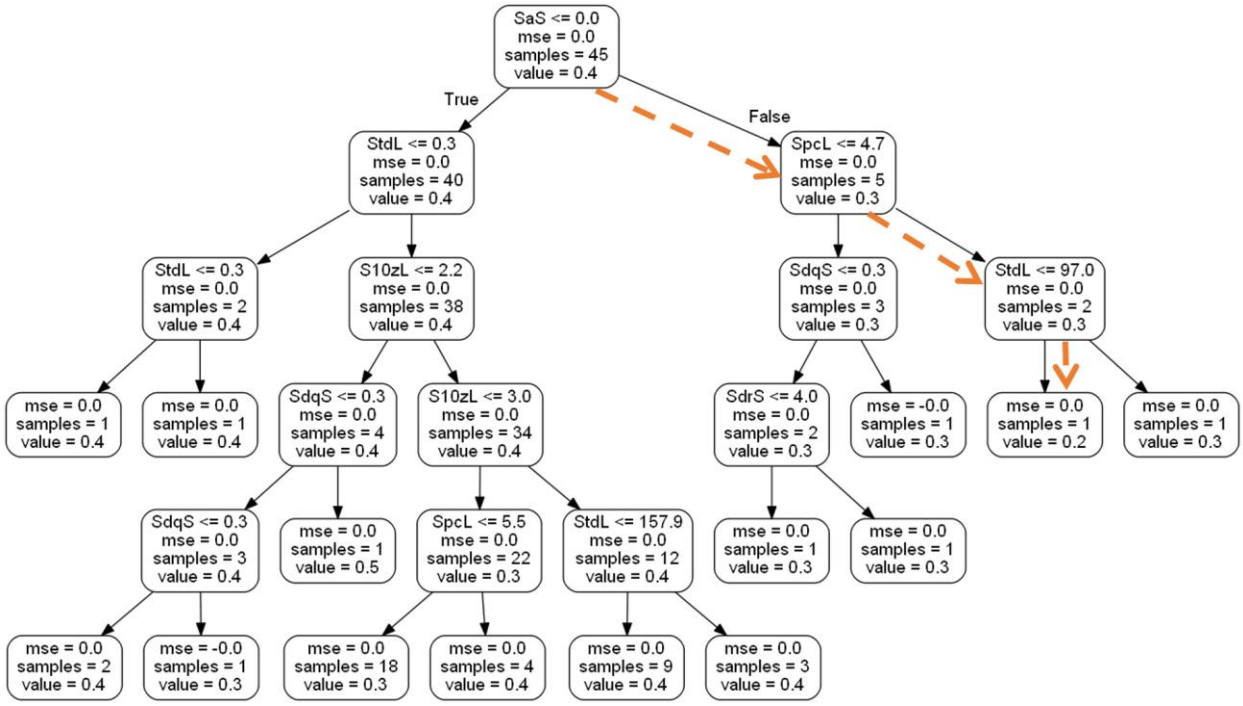

Figure 14 An Example Decision Tree in Random Forest

Friction Prediction Model

55 variables (27 pairs of 3D surface micro- and macro-texture indicators, and temperature) are used for developing friction prediction models at representative high and low speeds identified previously. 70% of the collected 108 pairs of pavement friction and their corresponding 55 variables are randomly selected for model development while the remaining 30% are used for model verification.

Model Development

Although the 55 variables provide a comprehensive list, their significances should be determined so that only the most significant ones can be maintained for friction model development. First, variable importance analysis is conducted via Python programming on the training data set for friction at the two representative speeds (70 and 15 km/h) using random forest algorithm. The top ranked variables are provided in decreasing order in Table 10. Model A specifies the friction predictive model at 70 km/h while Model B is for the friction predictive model at 15 km/h. The

importance value is a relative measurement. The sum of all the importance values of the significant variables in each model equals to one. The higher the importance value is, the stronger the link exists between the variables and the target. For instance, the most influential variable is Sa for micro-texture in Model A whereas it is the temperature in Model B.

Table 10 Variable Importance Analysis (Top 18 Variables)

Model A		Model B	
Variable	Importance Value	Variable	Importance Value
SaS	0.1113	Temperature	0.3221
SdqS	0.0726	VmcS	0.1441
S10zL	0.0557	VvcS	0.0427
SdrS	0.0538	StdS	0.0393
StrS	0.0413	SalL	0.0388
SpcL	0.0396	SalS	0.0344
Temperature	0.0372	SpcS	0.0322
StdL	0.0363	SdaL	0.0201
SskL	0.0341	SdqS	0.0145
SpL	0.0291	SpL	0.0135
S5vL	0.0272	S10zL	0.0131
SpcS	0.0266	SpcL	0.013
S5pL	0.0245	StdL	0.0119
SzL	0.0234	VvS	0.011
SdaL	0.0233	ShaL	0.0108
SalS	0.0208	SpdL	0.0108
StdS	0.0164	SdrS	0.0097
SvL	0.0164	StrS	0.0096

The top parameters with high importance values are selected to develop the friction prediction models. The optimal number of variables in the random forest model should be determined. Breiman (2001) recommended the number of variables in the model should be started at the integer less than $(1 + log_2 M)$, where M is the number of variables, which is 55 herein. Therefore, in the first attempt the top six $(1 + log_2 55)$ ranked variables are elected as inputs to build random forest regression models. Subsequently, one additional variable is added into the model and the goodness-of-fit is compared to the previous models. This process repeats until the best model is identified.

The R-squared value for the training data set is calculated to serve as a reference index for model determination. R-squared value is a statistical measure ranged from 0 to 1 that represents the proportion of the variance for targets that is explained by input variables. Commonly, the higher the R-squared value, the better the model fits the data. It is found that with the increasing of the number of variables, the R-squared value increases in the beginning but it tends to be steady afterwards. The optimal number of variables is seven for Model A with the R-squared value of 0.91, and eight for Model B with the R-squared value of 0.94. Table 11 lists the selected parameters which are used to predict friction performance.

Table 11 Random Forest Regression Model for Friction Prediction

Model	Items		Rank of Importance	Importance Value	Sum of Importance Value	Texture parameter Categories
High Speed Friction Model (70 km/h)	Micro-	Sa	1	0.183	0.488	Height
		Sdq	3	0.169		Hybrid
		Sdr	4	0.136		Hybrid
	Macro-	S10z	2	0.173	0.396	Feature
		Spc	5	0.129		Feature
		Std	7	0.094		Spatial
	Temperature		6	0.116	0.116	/
Low Speed Friction Model (15 km/h)	Micro-	Vmc	2	0.173	0.500	Functional
		Sal	3	0.099		Spatial
		Vvc	4	0.085		Functional
		Spc	6	0.073		Feature
		Std	7	0.071		Spatial
	Macro-	Sal	5	0.079	0.141	Spatial
		Sda	8	0.062		Feature
	Temperature		1	0.359	0.359	/

Pavement friction is composed of two principal forces: adhesion (depends mostly on micro-texture) and hysteresis (depends mostly on macro-texture) (Hall et al., 2009). Adhesion is the direct bonding/interaction between vehicle tire and micro-texture, while hysteresis is the energy loss due to tire deformation. The results herein indicate macro-texture exhibits a larger contribution to friction at 70 km/h (39.6%) than that at 15 km/h (14.1%). Hysteresis increases

along with the testing speed and becomes noticeably influential when the testing speed is above 105 km/h (Hall et al., 2009). Accordingly, micro-texture displays a significant contribution to fiction at both speeds. In addition, due to the viscoelastic properties of the testing tire material, hysteresis is affected by temperature and thus friction varies.

Model Verification

In this study, 70% of the collected data sets are randomly sampled for model development, while the remaining 30% for model verification. Using the developed friction models, the predicted friction numbers are calculated for the verification data set and compared with the measured friction at different speeds to validate the proposed models. The comparison results are shown in Figure 15. The R-squared values between the predicted and the measured friction numbers are 0.65 at 70 km/h and 0.67 at 15 km/h, indicating that over sixty percent of verification data can fit the proposed models.

In addition, the mean absolute errors (Equation (11)) and the accuracy (Equation (12)) are also calculated and shown in Figure 15. It can be concluded that the selected texture parameters are representative to predict pavement friction at both high and low speeds.

$$Mean\ Absolute\ Error = \frac{\sum |Predicted\ Friction - Measured\ Friction|}{number\ of\ predicted\ Friction} \qquad (11)$$

$$Accuracy = 100 - \frac{\sum(\frac{|Predicted\ Friction - Measured\ Friction|}{Measured\ Friction})}{Number\ of\ Predicted\ Friciton} \qquad (12)$$

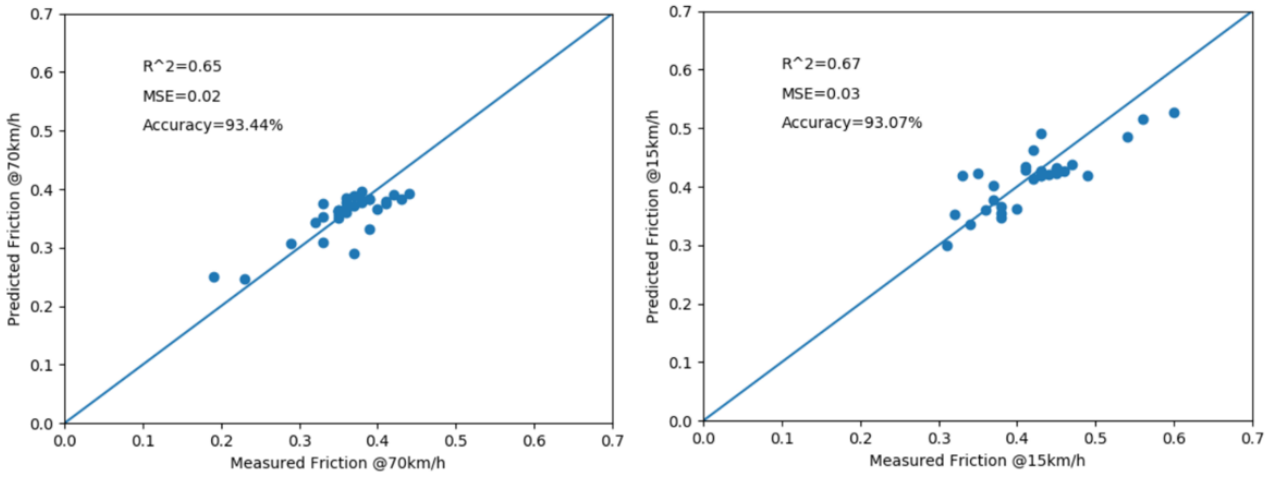

Figure 15 Model Verification

Conclusion

In this chapter, pavement friction prediction model has been developed and verified to have satisfactory performance at both high and low speeds. The results reveal that:

- 3D areal texture parameters of pavement surface at micro-scale play the most significant role in influencing pavement friction; Macro-texture is also significant for friction, while it exhibits a stronger contribution to friction numbers at high speed than at low speed.
- Temperature is significant for friction numbers at both high and low speeds.

The identified 3D texture parameters provide potential alternatives to describe the pavement texture in relation to friction performance. It also proposes new ways to evaluate pavement surface friction performance using high-resolution 3D data sets.

CHAPTER V

ENHANCED SAFETY PERFORMANCE FUNCTION FOR HIGHWAY SEGMENTS IN OKLAHOMA

Safety is one of the top priorities of the U.S. Department of Transportation (DOT). The safety performance functions (SPFs) are detailed as statistical models to predict the expected average crash frequency for a certain roadway facility, mainly as a function of traffic exposure indicators. Skid resistance is commonly agreed to have critical effects on highway safety, but have not been fully considered to estimate crash rates in current SPF in the Highway Safety Manual (HSM). In this chapter, skid resistance, along with roadway characteristics, is investigated and its contribution to vehicle crashes is explored. Furthermore, an enhanced safety performance function is developed by incorporating the significant influencing roadway characteristics for highway segments in Oklahoma.

Data Acquisition and Preprocessing

Factors contributing to roadway crashes can be classified into three general categories: human behavior, vehicle, and roadway/environment (HSM, 2010). This study only focuses on crashes where it is believed roadway is a contributing factor, while other categories are out of scope for this study. Factors in the roadway category include surface characteristics (e.g. skid resistance, IRI, Rut, etc.) and roadway geometry (e.g. grade, curvature, etc.). The relevant data for crash analysis has been collected and stored in various databases managed by ODOT, including the

PMS, SAFE-T database, Skid Studies Program, and SiteManager construction management system. Particularly, the investigated data and the data sources are summarized in Table 12.

Table 12 Data Sources for Crash Analysis

Data Item	Data Source
Crash data (frequency, type, severity)	SAFE-T
Average annual daily traffic (AADT)	
Presence of medians and shoulders	
Friction	Skid Studies Program
Segment identification: location, length	PMS
Pavement surface conditions: surface type, texture, IRI, rutting)	
Roadway geometry (grade, curve, number of lanes)	
Maintenance rehabilitation & reconstruction (MR&R) Works	SiteManager

Data Sources

Safety-T Database

SAFE-T is a database of statewide crash information garnered from collision report forms submitted by law enforcement (Adams and Warren, 2017). Data is available from 1998 to present. The database can generate reports in many formats based upon multiple criteria, including a range of dates and filters over the highway, control section, division, etc. Crash data is recorded as a point location event with a broad variety of relevant information.

Since crashes are rare and random events which naturally fluctuate over time at any given site (HSM, 2010), 5-year crash data was used in this study to decrease the risk of issues associated with crash fluctuation. Crash data on interstate, U.S. and state highways from 2012 to 2016 in the entire State of Oklahoma was acquired from the SAFE-T database. Meanwhile, relevant information was also obtained involving location information (highway name, control section number, mile point, subsection ID, GPS, etc.), collision type (rear-end, head-on, etc.), collision severity (fatality, injured, property damage, etc.), traffic in terms of AADT, and roadway data (shoulder, median, etc.).

Skid Studies Program

The Skid Studies Program at ODOT is managed through the Strategic Asset & Performance Management (SAPM) Division. ODOT used to perform systematic skid studies for the entire highway system, while in recent years the scope has been significantly downsized to only include annual testing of US-69, all Interstate Highways, as well as the Strategic Highway Research Program (SHRP) sites. In addition, ODOT also conducts special skid resistance testing as requested (ODOT, 2018).

ODOT collects friction data using a commonly used friction measurement equipment, locked-wheel skid tester operating at 50mph during testing. The friction data is recorded at an interval of approximately 0.5 miles and reported by control section saved as separate files. Significant preprocessing efforts are needed to combine those files into one universal database, since the scopes of testing sites have been changed during these years, and the reporting items and formats are not consistent.

In this study, friction data from 2012 to 2016 was gathered and summarized in Table 13. Friction is tested in one lane for each direction for divided roads, while one direction for undivided roads. The yearly skid testing is totaled from 0 to 5,078 lane-miles in the study period, yielding a total mileage of 18,341. No friction data was received in 2016, while only a handful of control sections on US-69 were tested in 2013.

Table 13 ODOT Skid Studies Program (2012-2016)

Year	Highway Classification	# of Control Section	Skid Testing Lane-miles
2012	I-35, US, SH	474	5,078
2013	US-69	14	213
2014	IS, US, SH	664	7,148
2015	IS, US, SH	553	5,903
2016	/	0	0
Total	IS, US, SH	1705	18,341

Pavement Management System (PMS)

ODOT PMS maintains a computer database of pavement distresses and other roadway characteristics on the National Highway System (NHS) and State Highway System (SHS) routes. It estimates the current and future needs of the NHS and SHS by producing a statewide annual report (ODOT, 2018).

The PMS data is collected on a 2-year cycle since 2001. About half of the mileage is collected in the first year, and the other half of the mileage is in the second year. The field data is formatted with one record for every 0.01 miles of pavement, including location information (highway name, control section number, mile point, control subsection, GPS, etc.), pavement surface characteristics (surface type, IRI, rutting, macro-texture, etc.), roadway geometry (grade, curvature, number of lanes, etc.), etc.

According to ODOT SAPM, the subsections of a control section are generated by multiple criteria based on ODOT Road Inventory Manual (OODT, 2010), such as state highway junction, political jurisdiction, urban area boundary, surface width or type change, et al. The subsection breaks are subject to change among different years if pavement type changes, or number of lanes changes, etc. More details on the breaking rules of control subsection can be found in ODOT Road Inventory Manual (OODT, 2010).

Table 14 Subsection in ODOT PMS Database (2012-2016)

Highway Classification	Year	# of Subsection	Avg Length of Subsection	Lane Miles
Interstate Highway	2012	0.00	0.00	0.00
	2014	1316.00	1.02	1346.00
	2016	1338.00	1.01	1346.00
United Highway	2012	771.00	0.91	702.00
	2014	1328.00	1.05	1397.00
	2016	491.00	0.86	421.00
State Highway	2012	198.00	1.11	221.00
	2014	184.00	1.14	211.00
	2016	0.00	0.00	0.00
Total		5626.00	1.00	5643.00

In this study, each subsection is considered as a uniform roadway segment for crash analysis. A brief summary of the PMS subsections from 2012 to 2016 is demonstrated in Table 14.

SiteManager Database

The ODOT Awarded Notices Highway Construction Contracts from 2012 to 2016 were obtained from the SiteManager system. The project and location description, project number, and allocated days were queried from the contracts and summarized to link to other data sets. The MR&R works that are considered to affect roadway crashes include changes of roadway geometry (widen median and shoulder alignment change etc.), pavement preventive maintenance, rehabilitation, and reconstruction.

Data Preprocessing

The acquired data was divided into roadway segments based on the subsections of a control section for later investigation in this study. First, a complete list of highway segments was generated for all the unique subsections from the ODOT PMS database, along with the starting and ending mile posts to define each segment. Subsequently, the initial list of segments was filtered by two criteria. Segments with missing roadway characteristics were eliminated, especially for those without friction data. Meanwhile, the segments with MR&R works during the analysis period were excluded to minimize the impacts of site conditions changes on roadway crashes.

Linking Various Database

The ability to associate all data for a given roadway segment is critical to the accurate and continued use of them for model development. A major challenge was the coordination of the various data sets using a common referencing system for processing the data efficiently. For one thing, SAFE-T crash data is referenced by control subsections with GPS coordinates, friction data is referenced by control section and milepost, PMS data contains both information, while the site

construction data only has descriptive location information that is manually collected from the ODOT Contract Section Maps. For another thing, data consistency issues continued to be a challenge facing many state highway agencies (SHAs). For example, the definitions of directions within the various databases are inconsistent. The PMS database uses "5" for primary directions while "6" for secondary directions of a roadway segment. The crash and friction data use letters to indicate the directions.

After manually modifying the inconsistent data to the same format, all required data was linked for each highway segment by subsection ID and direction of travel. As a result, the data size was reduced to 1835 segments. Furthermore, 24 segments were found to have MR&R works from 2012 to 2016, resulting in a final data size of 1811 segments. The basic information of the selected final list of segments is summarized in Table 15.

Table 15 Lane Miles Analyzed in Oklahoma (2012-2016) by Highway Class

Highway Classification	IS Hwy	US Hwy	State Hwy	Total
# of Segment	1103	587	121	1811
Average Segment Length	1.14	1.24	1.26	1.18
Lane Miles	1254	726.62	152.3	2132.93

SAFE-T Crash Data

Crash data contains a wide range of types, however, only vehicle crashes that are related to roadway characteristics were included in this study. For example, vehicle-train, vehicle-pedestrian, and vehicle-animal crashes were excluded. Crashes which involved alcohol, drugs, work zones, etc. were not considered in this study. Furthermore, crashes occurred on contaminated pavement conditions (snow, ice, oil, et al.), in which not enough contact between tire and pavement surface, have been eliminated from the analysis. After filtering and aggregating the crash data for the subsections, 34.5 % of the segments had no crashes during the analysis period. The detailed crash information is displayed in Table 16. The 5-year crash data of analysis

shows that 29.50% of the crashes led to fatalities or injuries, while 70.50% are property damage crashes. On average, 83.88% of crashes occurred on dry conditions and 16.12% on wet surfaces.

Table 16 Crashes Analyzed in Oklahoma (2012-2016) by Highway Class

Highway Class	IS Hwy	US Hwy	State Hwy	Total	%
Total Crash	25,941	3,644	454	30,039	100.00%
Crash Severity					
Fatal	135	52	7	194	0.65%
Personal Injury	7,369	1,126	172	8,667	28.85%
Property Damage	18,437	2,466	275	21,178	70.50%
Pavement Condition					
Dry	21,652	3,131	413	25,196	83.88%
Wet	4,289	513	41	4,843	16.12%
Type of Crash					
Fixed-Objects	5,600	638	99	6,337	21.10%
Sideswipe	4,779	434	34	5,247	17.47%
Angle-Related	2,532	1,125	146	3,803	12.66%
Rollover	893	137	29	1,059	3.53%
Head-On	49	35	4	88	0.29%
Rear End	12,088	1,275	142	13,505	44.96%

Safety-Related Data Sets

Several factors appear to influence roadway safety performance in previous studies (HSM, 2010; Arhin et al., 2015; Fwa et al., 2016; Aram, 2010; Miller and Zoloshnja, 2009), including traffic volume (AADT), roadway surface conditions (friction, texture, surface type, roughness), and geometry factors (longitudinal grade, horizontal curvature, number of lanes, presence of shoulder and median). These factors, available in the ODOT databases, are acquired and linked to each corresponding segment.

The surface type under this study include asphalt (AC), jointed concrete (JCP), and continuously reinforced concrete pavement (CRCP). For each segment, friction performance was measured by two indices: the average number and the interquartile range (IQR) of friction. IQR is the difference between the 75th and 25th percentiles of data, which is a statistical measurement of

variability. For surface texture, the average of the lowest quartile of mean profile depth (MPD) are used.

International roughness index (IRI), generally expressed in inch per mile, is a standard measure of the reaction of a vehicle to roadway profile and roadway roughness. FHWA (1990) recommended a threshold of 170 in/mile (2.7 m/km) for acceptable ride quality and a threshold of 95 in/mile (1.5m/km) for good ride quality. Accordingly, IRI is ranked as "Good", "Acceptable", or "Poor" for each of the 0.01-mile ODOT PMS data, and the lowest ranking level within the subsection is assigned to the segment.

Table 17 Contributing Factors for Crash Analysis

Factors		Description	Statistical Distribution
Crash Exposure	Segment Length	Segment Length (mile)	Min.: 0.05; Max.: 10.2; Mean: 1.178
	AADT	AADT(vehicle/day)	Min.: 1600; Max.:158,561; Mean: 28,653
	Rural or Urban	1-Rural; 2-Urban	Rural: 55.5%; Urban: 44.5%
Skid Resistance	Average Friction	The average friction value	Min.: 16.9; Max.: 62.0; Mean: 40.13
	IQR of Friction	Interquartile of friction	Min.: 0; Max.: 26.95; Mean: 2.85
	MPD	The average of lowest quartile MPDs	Min.: 0.336; Max.: 2.524; Mean: 0.766
Surface Conditions	Avg. IRI Ranking	1-Good; 2-Acceptable; 3-Poor	Good: 4.8%; Acceptable: 19.8%; Poor: 75.4%
	Max. Rut Ranking	1-Good; 2-Acceptable; 3-Poor	Good: 6.4%; Acceptable: 23.3%; Poor: 70.3%
	Pavement Type	1-AC; 2-JCP; 3-CRCP	AC: 57.8%; JCP: 30.6%; CRCP: 11.7%
Roadway Geometry	Avg. Grade	Average grade value	Min.: 0.033; Max.: 4.516; Mean: 1.013
	Average degree of curve	Average degree of curve	Min.: 0; Max.:17.293; Mean: 0.266
	Maximal degree of curve	The largest degree of curve	Min.: 0; Max.: 66.62; Mean: 1.188
	Length of curves	Total length of curves with radius < 1000 (m)	Min.: 0; Max.: 2.95; Mean: 0.103
	Number of Lanes	# of lanes	2, 3, 4, 6, 8, 10
	Presence of Shoulder	0-No; 1-Yes	No: 4.1%; Yes: 95.9%
	Presence of Median	0-No; 1-Yes	No: 10.7%; Yes: 89.3%

Rutting is a common distress along the two pavement wheel paths and presents a safety risk to vehicles during wet weather with reduced skid resistance, which could lead to loss of control or hydroplaning accidents (Fwa et al. 2016). Per literature review (AASHTO, 1989; Lister and Addis, 1977; Sousa et al. 1991), in this study a rut depth of 0.5 in (12.7mm) is selected as the threshold between high and medium rut severity, and 0.25 (6.4mm) is chosen in between medium and low rut severity. Similar to that for IRI, the most serious level is assigned to each corresponding segment.

Many research efforts have revealed the radius of the horizontal curve is significant for roadway crashes (Krammes et al. 1993; Aram, 2010). Studies have shown the difference between straight sections and curves becomes pronounced at a radius of about 1000m (Department of Transportation, 1984). Therefore, in this study, curves with radius below 1000m, or degree of curvature greater than 1.75°, are considered to have negative effects on safety. The total length of such curves within each segment is calculated for crash analysis.

The influencing factors and their descriptive statistics are shown in Table 17.

Development of Enhanced Safety Performance Function

Overview of Crash Modeling Methods

The crash prediction model (i.e. SPF) requires statistical analysis to map the relationship between crash data and roadway characteristics. Prior to the analysis, it is critical to understand the distribution of crash data. Crash occurrences are discrete and non-negative integers as well as random and rare events. Therefore, roadway safety in terms of the frequency of crashes is often studied, which involves the number of crashes occurring in some geographical space (usually a homogeneous roadway segment or intersection) over a specified time period.

Because crash-frequency data are non-negative integers, Poisson regression model has been used for analysis for several decades (Lord and Mannering, 2010). In a Poisson regression model, the probability of roadway segment i having y_i accidents per time period (5 years in this study) is given by:

$$P(y_i)=exp(-\lambda_i)\lambda_i^{y_i}/y_i! \quad (13)$$

Where, λ_i is the Poisson parameter for segment i, which equals to the expected number of accidents per time period in segment i. Poisson regression model is estimated by specifying the Poisson parameter λ_i as a function of explanatory variables, where the most common functional form being λ_i=exp (βX_i).

Although the Poisson model has been a commonly used approach for crash-frequency analysis, it restricts its distribution with equal mean and variance. Thus, it is not able to handle over-dispersion or under-dispersion problems, where the mean of the crash counts does not take the same value of the variance.

The Poisson-Gamma (Negative Binomial) regression model is an extension of the Poisson model to overcome such possible dispersion problems in the data. The Negative Binomial model introduces an error term (ϵ) into the Poisson parameter:

$$\lambda_i=exp\ (\beta X_i+\epsilon) \quad (14)$$

When ϵ approaches zero, the Negative Binomial model becomes a Poisson model. The addition term ϵ allows the variance of data to differ from the mean, as defined below with k as the over-dispersion parameter:

$$VAR(y_i)=E(y_i)+kE(y_i)^2 \quad (15)$$

In this study, the enhanced SPF is developed using negative binomial regression models with a log-linear relationship between crash frequency and roadway characteristics.

SPF and Empirical Bayes Method

SPFs are regression equations that estimate the average crash frequency for a specific site type. In HSM (2010), the SPFs have been developed for three facility types (rural two-lane roads, rural multilane highways, and urban and suburban arterials). An example SPF for roadway segments on rural two-lane highways is:

$$N_{SPFrs} = (AADT) \times (L) \times 365 \times 10^{-6} \times exp(-0.312) \quad (16)$$

Where, AADT is average annual daily traffic volume (vehicles per day) and L is the length of roadway segment (miles). Both factors are related to crash exposure, while roadway characteristics are not considered.

It is mandatory that the SPFs in the HSM be calibrated to local conditions since exiting SPFs are only directly representative of the sites used to develop them (HSM, 2010). Two parameters should be determined in calibration process: the calibration factor and calibrated dispersion parameter. The calibration factor (C) is determined by:

$$C = \sum_{all\ sites} observed\ crashes / \sum_{all\ sites} predicted\ crashes \quad (17)$$

Where, predicted crashes for each site are calculated using the SPF predictive model. Subsequently, the calibration factor works as a multiplier to the SPF prediction:

$$SPF_{Calibrated} = C * SPF_{existing} \quad (18)$$

Furthermore, the statistically reliability of average crash estimation can be improved by combining observed crash frequency and estimates of the average crash frequency, using the Empirical Bayes predictive method (EB Method) to compensate for the potential bias resulting from regression-to-the-mean (RTM). The RTM is the tendency of crash fluctuations where a comparatively high crash frequency is followed by a low crash frequency (Hauer, 1996). Failure to account for the RTM bias may result in an over- or under- estimation of long-term crash

frequency. The EB method uses a weighted adjustment factor, w, which is a function of the SPF's over-dispersion parameter, k, in the negative binomial distribution:

$$w = 1/(1 + k \times (\sum_{all\ study\ years} N_{predicted})) \quad (19)$$

Therefore, the expected average crash frequency for the analyzed period is:

$$N_{expected} = w \times N_{predicted} + (1 - w) \times N_{observed} \quad (20)$$

Selection of Influencing Factors

Variable selection is a process to determine a set of independent variables for the final regression model from a pool of candidate variables. On one hand, the subset of the independent variables needs to be as complete and realistic as possible. On the other hand, the independent variables included should be as few as possible to eliminate irrelevant variables, which will decrease the precision of the model as well as increase the complexity of data collection (NCSS). To balance the goodness-of-fit and model simplicity, the backward stepwise method is implemented for the model development.

The backward stepwise method is often used in variable selection for regression models. It starts with a model including all candidate variables. At each step, the variable with the least significance is removed until all the remaining variables are significant. To determine the best final model in this process, the Akaike Information Criterion (AIC) and the log-likelihood ratio test are performed. The AIC, proposed by Akaike (1973), has been used routinely during the past decades, which is calculated as below (Burnham and Anderson, 2002):

$$AIC = -2log(\mathcal{L}(\hat{\theta})) + 2K \quad (21)$$

where, $\log(\mathcal{L}(\hat{\theta}))$ is the maximized log-likelihood value and K is the number of estimable parameters in the approximating model. It is desired to rescale the AIC values so that the minimum AIC (AIC_{min}) has a value of zero. The AIC value can be rescaled as the simple difference:

$$\Delta_i = AIC_i - AIC_{min} \quad (22)$$

To better interpret the relative likelihood of a model, the Akaike weights is introduced as below:

$$w_i = exp(-\frac{1}{2}\Delta_i)/\sum_{r=1}^{R} exp(-\frac{1}{2}\Delta_i) \quad (23)$$

Subsequently, the model with the highest value is considered as the best model. Furthermore, the best model can be compared to other models by computing the evidence ratio:

$$ER_i = w_{best}/w_i \quad (24)$$

The evidence ratios help strengthen the evidence for or against the various alternative hypothesis. A large evidence ratio suggests a strong support that one model is better than the other.

Another technique to determine the best model is the log-likelihood ratio (LLR) test, which is generally used to compare two nested models where one model is obtained from the other by setting some of the parameters to be zero (PennState). The null hypothesis of this technique assumes the reduced model (L_r) is true. While the alternative hypothesis supposes the current model (L_c) is true. To test the null hypothesis, the likelihood-ratio is calculated using Equation 13 (Lord, et al., 2013) and compared with the Chi-Square critical value (χ_k^2). LLR is distributed as χ^2 statistic with k degree of freedom, where k is the difference in the number of parameters estimated between the two models including the intercepts (Lord et al., 2013). A larger LLR leads to small p-values, which indicates that the null hypothesis can be rejected. In other words, the reduced model is not preferred in comparison to the current model.

$$LLR = 2 \times (logL_r - logL_c) \quad (25)$$

Enhanced Safety Performance Function

Negative binomial regression model is developed using 5 years of statewide crash data in Oklahoma. The function form, as shown in Equation 26, is adopted to develop the enhanced SPF incorporating roadway characteristics. It should be noted that natural log transformation of segment length (L) and AADT are used herein:

$$N_{SPF} = \beta_1 L \times \beta_2 (AADT) \times exp(\alpha + \sum_3 \beta_i \times X_i) \quad (26)$$

Where: β_i = coefficient of the influencing variable Xi; α = intercept.

The initial model is built including all of the listed parameters in Table 17 and eliminating the least significant parameter step by step. The corresponding AIC is computed for each model and summarized in Table 18.

Table 18 Akaike Information Criterion for Model Selection

Model	AIC	Δ_i	w_i	ER_i	Variable Removed
1	10769.96	6.97	0.010	32.62	
2	10767.96	4.97	0.028	12.00	Max. Rut Level
3	10766.10	3.11	0.072	4.74	Smallest Quartile MPD
4	10764.38	1.39	0.170	2.00	Avg. Degree of Curve
5	10762.99	0.00	0.341	1.00	Length of Curve
6	10763.43	0.44	0.274	1.25	Rural or Urban
7	10766.10	3.11	0.072	4.74	Pavement Type
8	10767.99	5.00	0.028	12.18	Avg IRI Level
9	10772.47	9.48	0.003	114.43	Max. Degree of Curve
10	10779.20	16.21	0.000	3310.98	Avg Grade

The results of Akaike weights (w_i) in Table 18 indicate Model 5 has a 34.1% chance of being the best model, followed by Model 6 which eliminates an additional variable. The evidence ratio (ER_i) of Model 6 over Model 5 is 1.25, suggesting that Model 5 is 1.25 times more likely of being the best fit. Since the chances of being the best model are close for Model 5 and 6, the LLR test is performed to determine which model is to be used as the final model. As shown in Table 19, the p-value is greater than 0.05, failing to reject the null-hypothesis. In other words, including the extra variable does not provide significant improvement on the goodness-of-fit of the model. In conclusion, Model 6 is selected as the final SPF model in this study. The estimated coefficients and over-dispersion parameter are displayed in Table 20. The enhanced SPF model is obtained by inserting the coefficients into the model as shown in Equation 26.

Table 19 Log-Likelihood Ratio Test Results

Model	#Df	Chisq	Pr(>Chisq)	Results
6	13	2.4429	0.1181	Model 6 is a better model
5	14			

Table 20 Regression Analysis Results

Parameters	**Coefficients**	**Std. Error**	**z value**	**Pr(>|z|)**	
(Intercept)	-8.28	0.688	-12.037	< 2e-16	***
Segment Length	0.60	0.046	12.902	< 2e-16	***
AADT	1.24	0.066	18.767	< 2e-16	***
Avg Friction	-0.02	0.006	-2.455	0.0141	*
IQR Friction	-0.06	0.013	-4.667	3.1E-06	***
Avg IRI Level	0.16	0.072	2.259	0.0239	*
Pavement Type	-0.14	0.063	-2.159	0.0308	*
Avg Grade	0.20	0.066	3.051	0.0023	**
Max. Degree of Curve	0.03	0.011	2.410	0.0160	*
# of Lanes	0.19	0.051	3.733	0.0002	***
Presence of Shoulder	-1.37	0.196	-7.000	2.6E-12	***
Presence of Median	-0.93	0.164	-5.627	1.8E-08	***
	Signif. codes: 0 ‘***’ 0.001 ‘**’ 0.01 ‘*’ 0.05 ‘.’ 0.1 ‘ ’ 1				
	Dispersion parameter for Negative Binomial=0.4166				
	AIC: 10763.43				

In addition to segment length and AADT that are adopted in the AASHTO HSM SPF model, nine pavement surface conditions and roadway geometry factors are significant in contributing to roadway vehicle crashes. The positive regression coefficients for some factors, such as segment length, AADT, number of lanes, IRI level, degree of curvature of horizontal curves, and longitudinal grade, imply that the average risk of crashes is expected to increase with the increase of those factors. On the other hand, the risk of crashes will decrease by increasing the values of the rest condition factors with negative coefficients. It should be mentioned that both the average friction and the variance of friction (IQR) are significant to vehicle crashes.

Crash Estimation with Empirical Bayes Method

Because a crash is generally a rare event, one shortcoming of safety estimates based on accident counts is that they may be too imprecise to be useful. They are subject to a common, long

recognized, regression-to-mean (RTM) bias in safety analysis. For practical reasons, one is often interested in the safety of entities that either require attention because they seem to have too many accidents or merit attention because they have fewer accidents than expected. The Empirical Bayes (EB) method is commonly known to address two problems of safety estimation; it increases the precision of estimates beyond what is possible when one is limited to the use of two to three years of history accidents, and it corrects for the RTM bias.

With the enhanced SPF, the expected crash number in the five-year period is estimated combing with the EB method. An example is provided on US-69 and displayed in Figure 16. The figure displays the data by segments on US-69. The observed crash within each segment is marked with a triangle symbol, and the predicted crash from the SPF predictive model is plotted with circular circle symbols. In general, the estimation from the SPF model is found to be higher on those segments with zero observed crashes and lower than those segments with observed high crash rates. To reduce the RTM bias and produce more reliable crash estimations, the SPF predicted crash rate is further improved with the EB Method, as shown in Equations 19 and 20. After employing the EB method, the expected crash rate is plotted with a dotted black line in Figure 16.

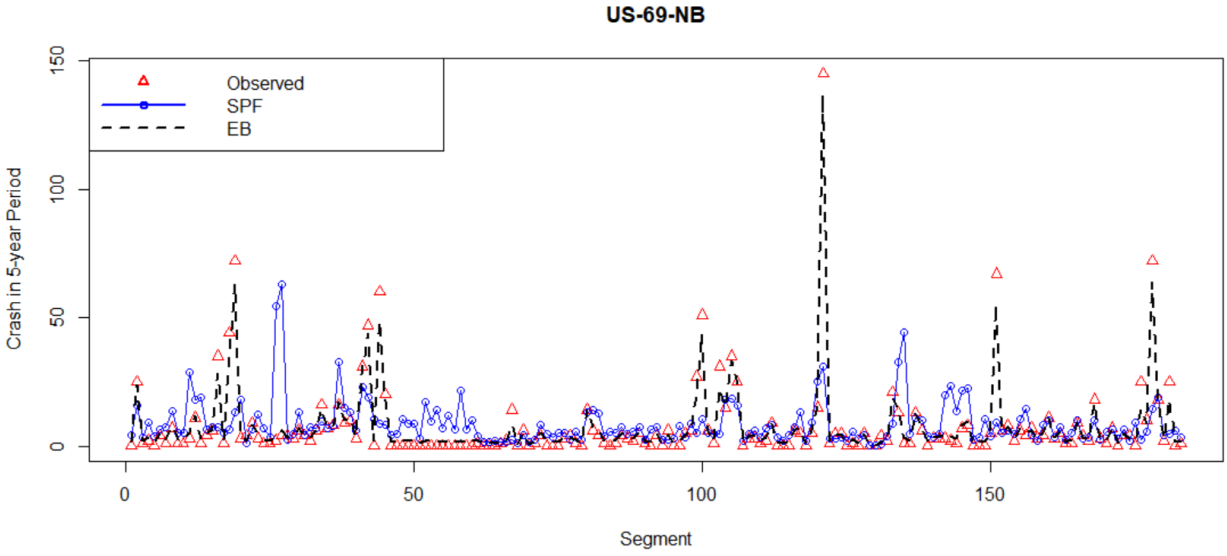

Figure 16 Observed, SPF Prediction, and Expected Crashes on US-69 NB

Conclusion

An enhanced safety performance function on statewide highway network in the State of Oklahoma has been developed in this study. In addition to the crash two exposure-related indicators (AADT and segment length), roadway characteristics are considered for SPF model development and crash analysis.

The average and variation of pavement friction and several other roadway factors, such as IRI level, grade and curvature, illustrate significant contributions to vehicle crashes. The expected risk of crashes may be reduced by improving surface friction, adding shoulder or median, and decreasing the grade or curvature. Furthermore, the statistical reliability of crash estimation is improved via Empirical Bayes (EB) method by combing observed crash data and predictions from the enhanced SPF.

The enhanced SPF could assist in better quantifying the influence of roadway characteristics on vehicle crashes. Before-after analysis can aid decision making to identify locations that may benefit the most from a safety treatment as well as to determine the most appropriate countermeasure.

CHAPTER VI

CONCLUSION

Findings

1. The Grip Tester based CFME measurements have sufficient repeatability to support the PFM program.
2. The Grip Tester based CFME measurement show a negative response to the change of temperature, testing speed and water film depth, while a positive response to the change of IRI.
3. HHT technique is feasible and useful for the extraction of meaningful pavement texture characteristics from pavement texture profiles, which could be correlate well to friction measurements. The friction model developed using operational parameters and the HT indicators can be used to adjust friction measurements at various testing conditions.
4. 3D areal texture parameters defined in the ISO 25178 can be deployed to characterize pavement texture information using high-resolution 3D texture data from pavement surfaces.
5. 3D areal pavement surface texture parameters at micro-scale paly more significant role in pavement friction than that from macro-texture and temperature. Macro-texture is also significant for friction, while it exhibits a stronger contribution to friction numbers at high speed than at low speed.
6. Temperature is significant for friction numbers at both high and low speeds.
7. Besides the two exposure indicators (traffic and segment length) used in the SPF in the

AASHTO HSM, many other roadway influencing factors, including pavement surface characteristics (friction, texture, IRI, rutting, pavement type) and roadway geometry (longitudinal grade, horizontal curvature, number of lanes, presence or absence of shoulder and median), are statistically significant to roadway safety and therefore are included in the enhanced SPF developed in this study. The expected risk of crashes may be reduced by countermeasures such as improving surface friction, adding shoulder or median, and decreasing the grade or curvature.

8. The expected risk of crashes may be reduced by improving surface friction, adding shoulder or median, and decreasing the grade or curvature.
9. The statistical reliability of crash estimation is further improved via Empirical Bayes method by combing historical crash data and predictions from the SPF.

Future Work

Further study could be focused on addressing the following problems:

1. The parameters from the HHT process could reflect the actual sharpness, power and curvature of the texture asperities at different scales, however thus far the mechanism on how they impact pavement skid resistance has not been fully understood.
2. This thesis studied the friction-related crashes of all severity levels (fatal, injured and property damaged), while crashes with high severity should be of interest particularly, such as single-fatal and multi-fatal crashes. The future research could compare the contributing factors of crashes with different severity levels, which will assist in well-informed decision makings to reduce crash severity and further improve roadway safety in Oklahoma.

REFERENCES

AASHTO. (1989). “Report of the AASHTO Joint Task Force on Rutting.” American Association of State Highway and Transportation Officials. Washington D.C.

AASHTO. (2008). “Guide for Pavement Friction, 1st Edition.” American Association of State Highway and Transportation Officials. Washington D.C.

Akaike, H. (1973). “Information theory and an extension of the maximum likelihood principle.” Second international symposium on information theory. pp. 267-281.

Anupam, K., Srirangam, S. K., Scarpas, A., and Kasbergen, C. (2013). “Influence of Temperature on Tire–Pavement Friction.” Transportation Research Record: Journal of the Transportation Research Board, 2369(1), 114-124. doi:10.3141/2369-13

Aram, A. (2010). “Effective Safety Factors on Horizontal Curves of Two-lane Highways.” Journal of Applied Sciences, 10(22), 2814-2822. doi:10.3923/jas.2010.2814.2822

Arhin, S. A., Noel, E. C., and Ribbiso, A. (2015). “Acceptable International Roughness Index Thresholds based on Present Serviceability Rating.” Journal of Civil Engineering Research, Vol. 5(4), 90-96. doi: 10.5923/j.jce.20150504.03

Association for Safe International Road Travel (ASIRT). (2018). “Road Safety Facts.” <http://web.archive.org/web/20181219165003/https://www.asirt.org/safe-travel/road-safety-facts/> (April 10, 2019)

ASTM. (2015). “Standard Specification for Standard Rib Tire for Pavement Skid-Resistance Tests.” E501-08. ASTM International, West Conshohocken, PA.

ASTM. (2015). “Standard Specification for Standard Smooth Tire for Pavement Skid-Resistance Tests.” E524-08. ASTM International, West Conshohocken, PA.

ASTM. (2015). “Standard Test Method for Friction Coefficient Measurements Between Tire and Pavement Using a Variable Slip Technique.” E1859/E1859m-11 (Reapproved 2015). ASTM International, West Conshohocken, PA.

ASTM. (2015). “Standard Test Method for Measuring the Skid Resistance of Pavements and Other Trafficked Surfaces Using a Continuous Reading, Fixed-Slip Technique.” E2340/E2340M-11. ASTM International, West Conshohocken, PA.

ASTM. (2015). “Standard Test Method for Skid Resistance of Paved Surfaces Using a Full-Scale Tire.” E274/E274M-15. ASTM International, West Conshohocken, PA.

ASTM. (2015). “Standard Test Method for Testing Side Force Friction on Paved Surfaces Using the Mu-Meter.” E670-09 (Reapproved 2015). ASTM International, West Conshohocken, PA.

ASTM. (2018). “Standard Test Method for Measuring Paved Surface Frictional Properties Using the Dynamic Friction Tester.” ASTM E1911-09a ASTM International, West Conshohocken, PA.

ASTM. (2018). “Standard Test Method for Measuring Surface Frictional Properties Using the British Pendulum Tester.” E3030-93 (Reapproved 2018). ASTM International, West Conshohocken, PA.

Austroads. (2005). “Guidelines for the management of road surface skid resistance.” AP-G83/05, Austroads, Sydney, NSW, Australia.

Austroads. (2009). “Guide to Asset Management Part 5F: Skid Resistance.” Austroads. Sydney, NSW, Australia. <https://austroads.com.au/publications> (May 23, 2019)

Austroads. (2011). “Review of Skid Resistance and Measurement Methods.” Austroads Project No. AT1488. Austroads, Sydney, NSW, Australia. ISBN 978-1-921709-73-9.

Ayenu-Prah, Y. and Attoh-Okine, N. O. (2009). "Comparative study of Hilbert–Huang transform, Fourier transform and wavelet transform in pavement profile analysis." Vehicle System Dynamics: International Journal of Vehicle Mechanics and Mobility, 47:4, 437-456

Bianchini, A., Heitzman, M., & Maghsoodloo, S. (2011). Evaluation of Temperature Influence on Friction Measurements. Journal of Transportation Engineering, 137(9), 640-647. doi:10.1061/(asce)te.1943-5436.0000271

Bledsoe J. (2015). "Missouri Demonstration Project: The Use of High-Friction Surface Treatments on Missouri Highways." FHWA, U.S. Department of Transportation.

Breiman, L. (2001). "Radom Forest," <http://web.archive.org/web/20181219165925/https://www.stat.berkeley.edu/~breiman/randomforest2001.pdf.> (April 12, 2019)

Breiman, L. (2002). "Manual on Setting Up, Using, and Understanding Random Forests V3.1." Statistics Department University of California Berkeley, CA, USA.

Burnham, K. P., and Anderson, D. R. (2002). "Model selection and multimodel inference: A Practical Information-Theoretic Approach, Second Edition." New York: Springer.

Chen, D., Han, S., Ye, A., Ren, X., Wang, W. and Wang, T. (2019). "Prediction of Tire-Pavement Friction based on Asphalt Mixture Surface Texture Level and Its Distributions." Road Materials and Pavement Design. DOI: 10.1177/1350650114544533.

Cho, C., Stoffels, S.M., Rado, Z. (2010). "Application of Hilbert Huang Transformation to analyze pavement texture-friction relationship." Thesis of the Pennsylvania State University.

De León Izeppi, E., Flintsch G. and McGhee K. (2010). "Field Performance of High Friction Surfaces." FHWA/VTRC 10-CR6. <http://www.virginiadot.org/vtrc/main/online_reports/pdf/10-cr6.pdf> (May 16, 2019)

De León Izeppi, E., Katicha, S. W., Flintsch, G. W., Mccarthy, R., and Mcghee, K. K. (2016). "Continuous Friction Measurement Equipment as a Tool for Improving Crash Rate Prediction: A Pilot Study." VTRC 16-R8, 2016. <http://www.virginiadot.org/vtrc/main/online_reports/pdf/16-r8.pdf> (May 17 2019)

Department of Transportation. (1984). "Highway Link Design Advice Note TA43/84." HMSO, London.

Ergun, M., Iyinam, S. and Iyinam A.F. (2005). "Prediction of Road Surface Friction Coefficient using Only Macro- and Microtexture Measurements." Journal of Transportation Engineering 131, no. 4, 10.1061/(ASCE)0733-947X(2005)131:4(311).

Federal Highway Administration (FHWA). (1990). "Highway Performance Monitoring System, Field Manual, Appendix J." FHWA Publication 5600.1A, U.S. Department of Transportation, FHWA, Washington, D.C.

Federal Highway Administration (FHWA). (2010). "Pavement Friction Management." Technical Advisory T 5040.38, U.S. Department of Transportation, FHWA, Washington, D.C. <https://www.fhwa.dot.gov/pavement/t504038.cfm#p01> (May 17, 2019)

Federal Highway Administration (FHWA). (2016). "Pavement Friction." U.S. Department of Transportation, FHWA, Washington, D.C. <https://safety.fhwa.dot.gov/roadway_dept/pavement_friction/> (April 1, 2019)

Federal Highway Administration (FHWA). (2018). "Federal Highway Administration (FHWA) Strategic Plan Fiscal Years 2019-2022." Report No. FHWA-PL-18-025, U.S. Department of Transportation, FHWA, Washington, D.C.

Federal Highway Administration (FHWA). (2019). "High Friction Surface Treatments (HFST)." U.S. Department of Transportation, FHWA, Washington, D.C. <https://safety.fhwa.dot.gov/roadway_dept/pavement_friction/high_friction/> (May 25, 2019)

Fernández-Blanco, E., Aguiar-Pulido, V., Robert Munteanu, C., and Dorado, J. (2013). “Random Forest Classification based on Star Graph Topological Indices for Antioxidant Proteins.” Journal of Theoretical Biology 317, pp331-337.

Flintsch, G., de León Izeppi, E., McGhee, K., and Najafi, S. (2010). “Speed adjustment factors for locked-wheel skid trailer measurements.” Transportation Research Record: Journal of the Transportation Research Board, No. 2155, Transportation Research Board of the National Academies, Washington, D.C. pp. 117–123.

Flintsch, G.W., McGhee, K.K., de León Izeppi, E., and Najafi, S. (2012). “The Little Book of Tire Pavement Friction” <http://web.archive.org/web/20181219165150/https://www.apps.vtti.vt.edu/1-pagers/CSTI_Flintsch/The%20Little%20Book%20of%20Tire%20Pavement%20Friction.pdf > (January 5, 2019)

Fwa, T. F., Chu, L., & Tan, K. H. (2016). “Rational Procedure for Determination of Rut Depth Intervention Level in Network-Level Pavement Management.” Transportation Research Record: Journal of the Transportation Research Board, 2589(1), 59-67. doi:10.3141/2589-07

Gagarin, N., Huang, E. N., Oklard, S. M., Sixbey, G. D., and Mekemson, R. J. (2004). “The application of the Hilbert-Huang transform to the anlysis of inertial profiles of pavements.” Int. J. Vehicle Design, Vol. 36, Nos. 2/3.

Geron, A. (2017). “Ensemble Learning and Random Forests,” in Hands-on Machine Learning with Scikit-learn & TensorFlow (Sebastopol, CA: O’Reilly Median, 2017), 181-202.

Hall, J.W., Smith, K.L., and Littleton, P. (2008). “Texturing of Concrete Pavements,” Final Report. Appendixes A-F. Applied Research Associates, Inc. <http://web.archive.org/web/20181219165245/http://onlinepubs.trb.org/onlinepubs/nchrp/nchrp_rpt_634appendixes.pdf.> (December 12, 2018)

Hall, J.W., Smith, K.L., Titus-Giover, L., Wambold, J.C., Yager, T.J., and Rado, Z. (2009). "NCHRP Web Document 108: Guide for Pavement Friction." NCHRP Project 01-43.

Hauer, E. (1996). "Statistical Test of Difference between Expected Accident Frequencies." Transportation Research Record. Journal of the Transportation Research Board, 1542(1), 24-29. https://doi.org/10.1177/0361198196154200104

Henry, J. J. (2000). "NCHRP Synthesis 291: Evaluation of Pavement Friction Characteristics." Transportation Research Board. National Academy Press, Washington, D.C.

Highway safety manual. (2010). American Association of State Highway and Transportation Officials. Washington, D.C.

Howell, D.C. (1998). "Statistical methods in human sciences." Wadsworth, New York.

Huang, N. E., Shen, Z., Long, S. R., Wu, M. C., Shih, H. H., Zheng, Q., Yen, N.-C., Tung, C. C. and Liu, H. H. (1998). "The Empirical Mode Decomposition and Hilbert Spectrum for Nonlinear and Nonstationary Time Series Analysis." Proceedings of the Royal Society London A., 454:903–995.

Hutengs, C., and Vohland, M. (2016). "Downscaling Land Surface Temperatures at Regional Scales with Random Forest Regression," Remote Sens. Environ. 178, (March 2016):127–141, http://dx.doi.org/10.1016/j.rse.2016.03.006

ISO 25178-2. (2012). "Geometrical product specifications (GPS) — Surface texture: Areal - Part 2: Terms, definitions and surface texture parameters." International Organization for Standardization (ISO).

Kanafi, M.M., Kuosmanen, A., Pellinen, T. K., and Tuononen, A. J. (2015). "Macro- and Micro-Texture Evolution of Road Pavements and Correlation with Friction." International Journal of Pavement Engineering 16, no. 2: 168-179, https://doi.org/10.1080/10298436.2014.937715.

Kane, M., Rado, Z. and Timmons, A. (2015). “Exploring the texture–friction relationship: from texture empirical decomposition to pavement friction, International Journal of Pavement Engineering.” 16:10, 919-928. DOI: 10.1080/10298436.2014.972956

Karamihas, S.M. (2004). “Development of cross correlation for objective comparison of profiles”, Int. J. Vehicle Design, Vol. 36, Nos. 2/3, pp. 173-193.

Kargah-Ostadi, N. and Howard, A. (2015). “Monitoring Pavement Surface Macrotexture and Friction-Case Study.” Transportation Research Record: Journal of the Transportation Research Board 2525, pp. 111-117.

Katicha, S.W., Mogrovejo, D.E., Flintsch, G.W., and de León Izeppi, E.D (2015). “Adaptive Spike Removal Method for High-Speed Pavement Macrotexture Measurements by Controlling the False Discovery Rate.” Transportation Research Record: Journal of the Transportation Research Board, vol. 2525, pp. 100–110., doi:10.3141/2525-11.

Kogbara, R.B., Masad, E.A. Kassem, E., Scarpas, A. and Anupam, K. (2016). “A State-of-the-art Review of Parameters Influencing Measurement and Modeling of Skid Resistance of Asphalt Pavements.” Construction and Building Materials 114, pp. 602-617, https://doi.org/10.1016/j.conbuildmat.2016.04.002.

Krammes, R.A., Braker, R.Q., Shafer, M.A., Ottesen, J.L., Anderson, I.B., Fink, K. L., Collins, K. M., Pendleton, O. J., and Messer, C. J. (1993). “Horizontal alignment design consistency for rural 2-lane highways.” Report No. FHWA-RD94-034.

Leach R. (2012). “Characterisation of Areal Surface Texture.” Springer-Verlag Berlin Heidelberg. https://doi.org/10.1007/978-3-642-36458-7.

Li, Q., Yang, G., Wang, K., Zhan, Y., and Wang, C. (2017). “Novel Macro- and Microtexture Indicators for Pavement Friction by Using High-Resolution Three-Dimensional Surface Data.” Transportation Research Record: Journal of the Transportation Research Board 2641, pp. 164–176. http://dx.doi.org/10.3141/2641-19

Li, S., Noureldin, S., and Zhu, K. (2004). “Upgrading the INDOT Pavement Friction Testing Program.” FHWA/IN/JTRP-2003/23. Indiana Department of Transportation and Purdue University, West Lafayette, Indiana.

Li, S., Noureldin, S., Jiang, Y., and Sun, Y. (2012). “Evaluation of Pavement Surface Friction Treatments.” Report: FHWA/IN/JTRP-2012. DOI: 10.5703/1288284314663

Li, S., Noureldin, S., Zhu, K., and Jiang, Y. (2012). “Pavement Surface Microtexture: Testing, Characterization, and Frictional Interpretation.” Pavement Performance: Current Trends, Advances, and Challenges, pp59–76. https://doi.org/10.1520/STP104426.

Li, S., Zhu, K. and Noureldin, S. (2007). “Evaluation of Friction Performance of Coarse Aggregates and Hot-Mix Asphalt Pavements.” Journal of Testing and Evaluation, Vol. 35, No. 6, 1-7. Paper ID JTE100903

Lister, N. W., and Addis. R. R. (1977). “Field Observations of Rutting and Practical Implications.” Transportation Research Record 640, pp. 28–34, TRB, National Research Council, Washington, D.C.

Lord, D., and Mannering, F. (2010). “The statistical analysis of crash-frequency data: A review and assessment of methodological alternatives.” Transportation Research Part A: Policy and Practice, 44(5), 291-305. doi:10.1016/j.tra.2010.02.001

Lord, D., Park, B.J. and Levine, N. (2013). “Chapter 16: Poisson Regression Modeling.” CrimeStat IV: A Spatial Statistics Program for the Analysis of Crime Incident Locations, Version 4.0. Ned Levine and Associates, Houston, TX, and Washington, D. C.

Louppe, G., Wehenkel, L., Sutera, A., and Geurts, P. (2013). “Understanding Variable Importances in Forests of Randomized Trees.” Advances in Neural Information Processing Systems 26 NIPS 2013, Dept. of EE & CS, & GIGA-R Universit´e de Li`ege, Belgium.

Lu, J., A. Gan, K. Haleem, P. Alluri, and K. Liu. (2012). “Comparing Locally-Calibrated and Safety-Analyst Default Safety Performance Functions for Florida’s Urban Freeways.” Presented at the 91st Annual Meeting of the Transportation Research Board, Washington, D.C.

Lyon, C., Persaud, B., and Gross, F. (2016). “The Calibrator-An SPF Calibration and Assessment Tol User Guide.” Report No. FHWA-SA-17-016.

Masad, E. (2005). “Aggregate Imaging System (AIMS): Basics and Applications.” FHWA/TX-05/5-1707-01-1, Texas Transportation Institute, College Station, Texas.

Merritt, D.K., Lyon, C.A., and Persaud, B. N. (2015). “Evaluation of Pavement Safety Performance.” FHWA-HRT-14-065.

Miller, T. R., and Zaloshnja, E. (2009). “On a crash course: The dangers and health costs of deficient roadways.” Transportation Construction Coalition. Washington, D.C.

Moore, D.F. (1966). “Prediction of Skid-Resistant Gradient and Drainage Characteristics of Pavements.” Highway Research Record 131, Highway Research Board, Washington, D.C., pp. 181-203.

Najafi, S, Flintsch, G.W., de Leon Izeppi, E. D., McGhee, K. and Katicha, S. (2017). “Evaluation of repeatability and reproducibility of continuous friction measuring equipment (CFME) using cross-correlation.” International Journal of Pavement Engineering, 18:6, 521-529, DOI: 10.1080/10298436.2015.1095908

Najafi, S., Flintsch, G.W., and Medina, A. (2017). “Linking Roadway Crashes and Tire-Pavement Friction: A Case Study,” International Journal of Pavement Engineering 18, no. 2: 119-127, https://doi.org/10.1080/10298436.2015.1039005.

NCSS Statistical Software. “Chapter 311-Stepwise Regression.” <https://ncss-wpengine.netdna-ssl.com/wp-content/themes/ncss/pdf/Procedures/NCSS/Stepwise_Regression.pdf> (April 23, 2019)

ODOT. (2018). “ODOT State Planning and Research Work Program FFY2019”. Oklahoma Department of Transportation. p. 18, p. 25.

PennState Eberly College of Science. (2018). “STAT 504, 6.2.3-More on Goodness-of-Fit and Likelihood Ratio Tests.” <https://newonlinecourses.science.psu.edu/stat504/node/220/> (April 23, 2019)

Qian, Z. and Meng, L. (2017). “Study on Micro-Texture and Skid Resistance of Aggregate during Polishing,” Front. Struct. Civ. Eng. 11, no. 3, pp. 346-352, https://doi.org/10.1007/s11709-017-0409-7.

Rado, Z. and Kane. M. (2014). “An initial attempt to develop an empirical relation between texture and pavement friction using the HHT approach.” Wear, Volume 309, Issues 1-2, pp. 233-246. https://doi.org/10.1016/j.wear.2013.11.015

Roe, P. G., and Sinhal, R. (1998). "The Polished Stone Value of aggregates and in-service skidding resistance." TRL Report 322, TRL, Crowthorne, UK.

Salem, O., Liu, Y., and Mehaoua, A. (2013). “A lightweight Anomaly Detection Framework Medical Wireless Sensor Networks.” 2013 IEEE Wireless Communications and Networking.

Serigos, P.A., Smit, A.F. and Prozzi, J. (2014). “Incorporating Surface Microtexture in the Prediction of Skid resistance of Flexible Pavements,” Transportation Research Record 2457, pp. 105-113, DOI: 10.3141/2457-11.

Sousa, J. B., Craus, J. and Monismith, C. L. (1991). “SHRP Report A/IR-91-104: Summary Report on Permanent Deformation in Asphalt Concrete.” TRB, National Research Council, Washington, D.C.

Srinivasan, R., Carter, D., and Bauer, K. (2013). “Safety Performance Function Decision Guide: SPF Calibration vs SPF Development.” Report No. FHWA-SA-14-004.

VicRoads (2018). “Technical Note 110: Measurement and Interpretation of Skid Resistance using SCRIM.” Victoria, Australia.

Wallman, C. G., and Astrom, H. (2001). “Friction measurement methods and the correlation between road friction and traffic safety: A literature review.” Linköping, Sweden: Swedish National Road and Transport Research Institute (VTI). pp. 42.

World Road Association (PIARC). (1987). “Report of the Committee on Surface Characteristics,” Proceedings of the XVIII World Road Congress. Paris, France.

Yang, G., Li, Q., Zhan, Y., and Wang, K. (2017). “Field Monitoring of the Long Term Pavement Performance (LTPP) Warm-Mix Asphalt (WMA) Site in Oklahoma.” 2017 International Conference on Transportation Infrastructure and Materials (ICTIM 2017). https://doi.org/10.12783/dtmse/ictim2017/9906.

Zahir, H., Islam, S., and Hossain, M. (2017). “Friction Management on Kansas Department of Transportation Highways.” Report No. K-TRAN: KSU-14-5.

Zuniga-Garcia, N. and Prozzi, J.A. (2016). “Contribution of Micro- and Macro-Texture for Predicting Friction on Pavement Surfaces,” CHPP Report-UTA#3-2016, Michigan State University, Okemos, MI.

VITA

Wenying Yu

Candidate for the Degree of

Master of Science

Thesis: CHARACTERING PAVEMENT SKID RESISTANCE FOR ROADWAY CRASH PREDICTION IN OKLAHOMA

Major Field: Civil Engineering

Biographical:

Education:

Completed the requirements for the Master of Science in Civil Engineering at Oklahoma State University, Stillwater, Oklahoma in July, 2019.

Completed the requirements for the Bachelor of Science in Civil Engineering at Oklahoma State University, Stillwater, Oklahoma in 2017.

Experience:

Graduate Research Assistant, Department of Civil and Environmental Engineering, Oklahoma State University, August 2017 to present.

Podium presentation at the 15th Annual Interuniversity Symposium on Infrastructure Management (AISIM) at the Rutgers University, Piscataway, NJ in May, 2019.

Podium and poster presentations at the Southern Plains Transportation Center (SPTC) 2018 Summer Symposium at Metro Tech Conference Center, Oklahoma City, OK in August, 2018.

Publications and Papers:

Guangwei Yang, **Wenying Yu**, Joshua Qiang Li, Kelvin C.P. Wang, and Peng Yi (2019). Random Forest based Pavement Surface Friction Prediction Using High Resolution 3D Image Data. *Journal of Testing and Evaluation*. doi.org/10.1520/JTE20180937

Guangwei Yang, Joshua Qiang Li, You Zhan, **Wenying Yu**, Kelvin C.P. Wang, and Yi Peng (2019). Field Performance of High Friction Surface Treatments (HFST) in Oklahoma. *Canadian Journal of Civil Engineering.* doi.org/10.1139/cjce-2018-0521